Five millennia of mitochondrial introgression in Atlantic bluefin tuna identified using ancient DNA

Emma Falkeid Eriksen[1*], Adam Jon Andrews[1,2,3], Svein Vatsvåg Nielsen[4], Per Persson[5], Estrella Malca[6,7], Vedat Onar[8], Veronica Aniceti[9], Gäel Piquès[10], Federica Piattoni[3], Francesco Fontani[11], Martin Wiech[12], Keno Ferter[12], Oliver Kersten[1], Giada Ferrari[1], Alessia Cariani[3], Fausto Tinti[3], Elisabetta Cilli[11], Lane M. Atmore[1], Bastiaan Star[1*]

[1] Centre for Ecological and Evolutionary Synthesis (CEES), Department of Biosciences (IBV), University of Oslo, Norway
[2] Norwegian Institute of Water Research, Oslo, Norway
[3] Department of Biological, Geological and Environmental Sciences, University of Bologna, Ravenna, Italy
[4] Stavanger Maritime Museum, Stavanger, Norway
[5] Museum of Cultural History, University of Oslo, Norway
[6] Cooperative Institute for Marine and Atmospheric Studies, University of Miami, Miami, Florida, United States of America
[7] NOAA Fisheries, Southeast Fisheries Science Center, Miami, Florida, United States of America
[8] Osteoarchaeology Practice and Research Centre, Faculty of Veterinary Medicine, Istanbul University-Cerrahpaşa, Istanbul, Türkiye
[9] Museum of Natural History, University of Bergen, Bergen, Norway
[10] ASM, CNRS, Université Paul Valéry-Montpellier 3, Montpellier, France
[11] Department of Cultural Heritage, University of Bologna, Ravenna, Italy
[12] Institute of Marine Research, PO Box 1870, N-5817 Bergen, Norway

*Corresponding authors: emeriks@uio.no, bastiaan.star@ibv.uio.no

Abstract

Mitogenomic (MT) introgression between species is readily documented in marine fishes. Such introgression events may either be long-term natural phenomena or the result of human-driven shifts in spatial distributions of previously separated species. Determining the drivers behind MT introgression is stymied by the difficulty of directly observing patterns of interbreeding over long timescales. Using ancient DNA spanning five millennia, we here investigate the long-term presence of MT introgression from Pacific bluefin tuna (*Thunnus orientalis*) and albacore (*Thunnus alalunga*) into Atlantic bluefin tuna (*Thunnus thynnus*), a species with extensive exploitation history and observed shifts in abundance, and demographic distribution. Comparing ancient (n=130) and modern (n=78) mitogenomes of specimens covering most of the range of Atlantic bluefin tuna we detect no significant spatial or temporal population structure. This lack of spatiotemporal genomic differentiation is indicative of ongoing gene flow between populations and large effective population sizes over millennia. Moreover, we identify introgressed MT genomes in ancient specimens up to 5000 years old and find that this rate of introgression has remained similar through time. We therefore conclude that MT introgression in the Atlantic bluefin tuna is to date unaffected by anthropogenic impacts. By providing the oldest example of directly observed MT introgression in the marine environment, our results highlight the utility of ancient DNA to obtain temporal insights in the long-term persistence of such phenomena.

Introduction

Genetic introgression is the integration of genetic material from one parent species into another following interspecific hybridization and backcrossing (Rhymer & Simberloff, 1996). Although frequency of the phenomenon across biological systems remains debated, the increased use of next-generation sequencing across non-model taxa has revealed introgression to be a more common phenomenon in nature than previously thought (Dagilis et al., 2022). The majority of documented introgression in animals involves introgression of the mitochondrial (MT) genome (Sloan et al., 2017; Pons et al., 2014; Toews & Brelsford, 2012). Typically inherited maternally in vertebrates, the non-recombining introgressed mitogenome remains largely intact over time (Seixas et al., 2018; Brown, 2008). The presence of introgressed MT haplotypes can cause significant bias when using mitogenomic data to describe a species demographic properties or evolutionary history. Even rare hybridization events can result in the presence of whole MT haplotypes that do not accurately reflect the typical history or

demography of the taxon. For example, the presence of introgressed MT haplotypes may dominate genealogies with recent dispersal history and thereby overshadow genetic signals from past dispersal events (Sloan et al., 2017; Ballard & Whitlock, 2004). Presence of introgressed, heterospecific alleles and haplotypes will also affect population genomic analyses by inflating measures of genetic diversity and divergence (Oosting et al., 2023; Rodriguez & Krug, 2022; Wang et al., 2022; Hawks, 2017). Avoiding such inflation is important because these statistics can influence management choices (Willi et al., 2022; Hohenlohe et al., 2021; Kardos et al., 2021) and inflated measures of genetic diversity or effective population size may exaggerate the genetic robustness of a truly vulnerable population.

Marine fish hybridize according to their ecologies and life history strategies, thus the rate of introgression will vary according to migration behavior, spawning site overlap, fecundity, spawning ontology, and offspring survival (Montanari et al., 2016; Gardner, 1997; Hubbs, 1955). In the economically important redfish (*Sebastes spp.*), high rates of introgressive hybridization (15% of all samples) have been found between two species (*S. fasciatus* and *S. mentella*) that live sympatrically in hybrid zones and yet maintain their morphology, resembling one of the parent species (Benestan et al., 2021; Roques et al., 2001). Likewise, introgression has been observed in European seabass (*Dicentrarchus labrax*) (Duranton et al., 2020; Vandeputte et al., 2019), capelin (*Mallotus villosus*) (Cayuela et al., 2020; Colbeck et al., 2011), European anchovy (*Engraulis encrasicolus*) (Le Moan et al., 2016), Australasian snapper (*Chrysophrys auratus*) (Oosting et al., 2023) and Atlantic and Pacific herring (*Clupea harengus* and *C. pallasii*) (Semenova, 2020).

Formation of hybrid zones after recent range shifts induced by contemporary climate change have already been observed in a number of species (Kersten et al. 2023; Ottenburghs, 2021; Garroway et al., 2010; Taylor & Larson, 2019; Ryan et al., 2018) including marine fish (Muhlfeld et al., 2014; Potts et al., 2014). The formation of such hybrid zones can have both deleterious and advantageous effects. For instance, in trout, warmer freshwater temperatures and lower precipitation is expected to increase introgressive hybridization between native European brown trout (*Salmo trutta*) and released non-native brown trout in Mediterranean rivers, potentially leading to loss of local genetic variants (Vera et al., 2023). Yet in rainbowfish (*Melanotaenia* spp.), it has been suggested that introgressive hybridization contributes to climate change resiliency by incorporating potentially adaptive genetic variation (Brauer et al., 2023; Turbek & Taylor, 2023). Regardless of the evolutionary consequences, knowledge about the *timing* of the introgression is necessary to understand if it is anthropogenic impacts that

increase rates of hybridization, thereby positively or negatively altering the adaptive potential of species (Xuereb et al., 2021; Hoffmann & Sgrò, 2011).

In this study, we investigate introgression in the ecologically and economically important Atlantic bluefin tuna (*Thunnus thynnus*, Linneaus 1758), a highly migratory marine predatory fish distributed across the Atlantic Ocean (SCRS, 2023; Block, 2019; Nøttestad et al., 2020). Atlantic bluefin exhibits strong natal homing behavior (Brophy et al., 2016; Boustany et al., 2008; Block et al., 2005) and is therefore managed as two separate stocks: the larger Eastern stock spawning predominantly in the Mediterranean, and a smaller Western stock spawning predominantly in the Gulf of Mexico (ICCAT, 2023). Recent studies, however, have demonstrated weak genetic divergence in Atlantic bluefin and the existence of a previously unknown spawning ground in the Slope Sea where the stocks seem to interbreed (Diaz-Arce et al., 2024; Aalto et al., 2023; Andrews et al., 2021; Rodríguez-Ezpeleta et al., 2019), thereby challenging the assumption of two reproductively isolated populations. After severe international overfishing of Atlantic bluefin in the last century, the Eastern Atlantic bluefin stock has at present efficiently recovered due to strict management measures and favorable oceanographic conditions in the recent decade (ICCAT 2022a, 2022b) followed by improved recruitment with a series of very strong year classes (Reglero et al. 2018; Garcia et al. 2013; ICCAT 2023). The Atlantic bluefin has an extensive exploitation history, starting in the early Neolithic (ca. 6000 BCE), expanding through the Greek and Roman era and developing into an intense fishing industry towards the end of the last millennium (Andrews et al., 2022). Consequently, Atlantic bluefin stocks were depleted by the 21st century (Block, 2019; MacKenzie et al., 2009), leading to shifts in its demographic distribution and foraging behavior (Di Natale, 2015; MacKenzie et al., 2014; Andrews et al., 2023a; Worm & Tittensor, 2011). These distributional changes, as well as the establishment of potentially new spawning grounds may affect the rate of introgression in the species by providing increased or decreased opportunities for hybridization.

MT introgression within the Thunnus genus has been well documented, and together with the lack of reliable phylogenetically informative markers to distinguish the species, contributed to an unresolved phylogeny within the genus until recently (Alvarado Bremer et al., 1997; Chow et al., 2006; Chow & Kishino, 1995; Díaz-Arce et al., 2016; Santini et al., 2013; Viñas & Tudela, 2009). The Atlantic bluefin was previously thought to be a subspecies of Northern bluefin tuna together with Pacific bluefin (*Thunnus orientalis,* Temminck and Schlegel 1844). The bluefins are now regarded as distinct species (Chow et al., 2006; Díaz-Arce et al., 2016) with non-overlapping ranges (Tseng et al., 2011) (see Figure S1). The Pacific

bluefin, distributed across the North Pacific Ocean, is closely related to albacore tuna (*Thunnus alalunga*, Bonnaterre 1788) in mitochondrial phylogenies (Gong et al., 2017; Viñas & Tudela, 2009; Chow et al., 2006). Albacore tuna is found in both the Pacific, Indian and Atlantic Oceans, including the Mediterranean Sea, typically preferring warmer waters than the Pacific and Atlantic bluefins, but with largely overlapping ranges and spawning areas (Chow & Ushiama, 1995; Saber et al., 2015). In the most recent and resolved nuclear phylogeny, the albacore tuna occurs as the sister-species to the other Thunnus species, and the Pacific and Atlantic bluefin form a monophyletic group (Díaz-Arce et al., 2016; Ciezarek et al. 2018) (see Figure S1).

MT introgression has been demonstrated from both albacore and Pacific bluefin into the Atlantic bluefin and from the Atlantic bluefin and albacore into the Pacific bluefin, but no MT introgression has been found in albacore (Alvarado Bremer et al., 2005; Carlsson et al., 2004; Chow & Kishino, 1995; Rooker et al., 2007; Viñas et al., 2003, 2011; Viñas & Tudela, 2009; Chow et al., 2006; Chow & Inoue, 1993). In the Atlantic bluefin, the rates of introgression from either albacore or Pacific bluefin are similar at around 2-5% (Rooker et al., 2007; Viñas & Tudela, 2009). Nonetheless, it is unclear when these introgression events started to occur or whether they are ongoing. In addition to the distributional shifts likely caused by high fishing pressures, it is possible that climate warming has contributed to novel opportunities for introgression in recent decades. The distribution of Atlantic bluefin over the last century has fluctuated with temperature (Faillettaz et al., 2019; Ravier & Fromentin, 2004), and ocean warming has been implicated in altering migration patterns, spawning ontology, and habitats of the Atlantic bluefin (Diaz-Arce et al., 2023; Faillettaz et al., 2019; Fiksen & Reglero, 2022; Muhling et al., 2011). Determining the timing of hybridization events can therefore shed light on the drivers of introgression.

DNA extracted from historical or ancient samples (hDNA or aDNA) allows us to directly investigate the timing of introgression events and to elucidate potential changes in population structure and genetic diversity over time (Kersten et al. 2023). Fish bones have physiological qualities that may increase the likelihood of finding well preserved DNA (Ferrari et al., 2021; Kontopoulos et al., 2019; Szpak, 2011) allowing for whole genome sequencing (Star et al., 2017), even from very limited amounts of bone (e.g. <10 mg) (Atmore et al., 2023). Here we use such aDNA methods to analyze mitogenomes from 130 ancient and 78 modern Atlantic bluefin spanning a period of approximately 5000 years (Figure 1). By sampling both before and after the period of heavy exploitation (1970-2007) and ongoing climate change, we

investigate spatiotemporal patterns of genetic diversity and provide the longest historical time series of the presence of MT introgression in the marine environment to date.

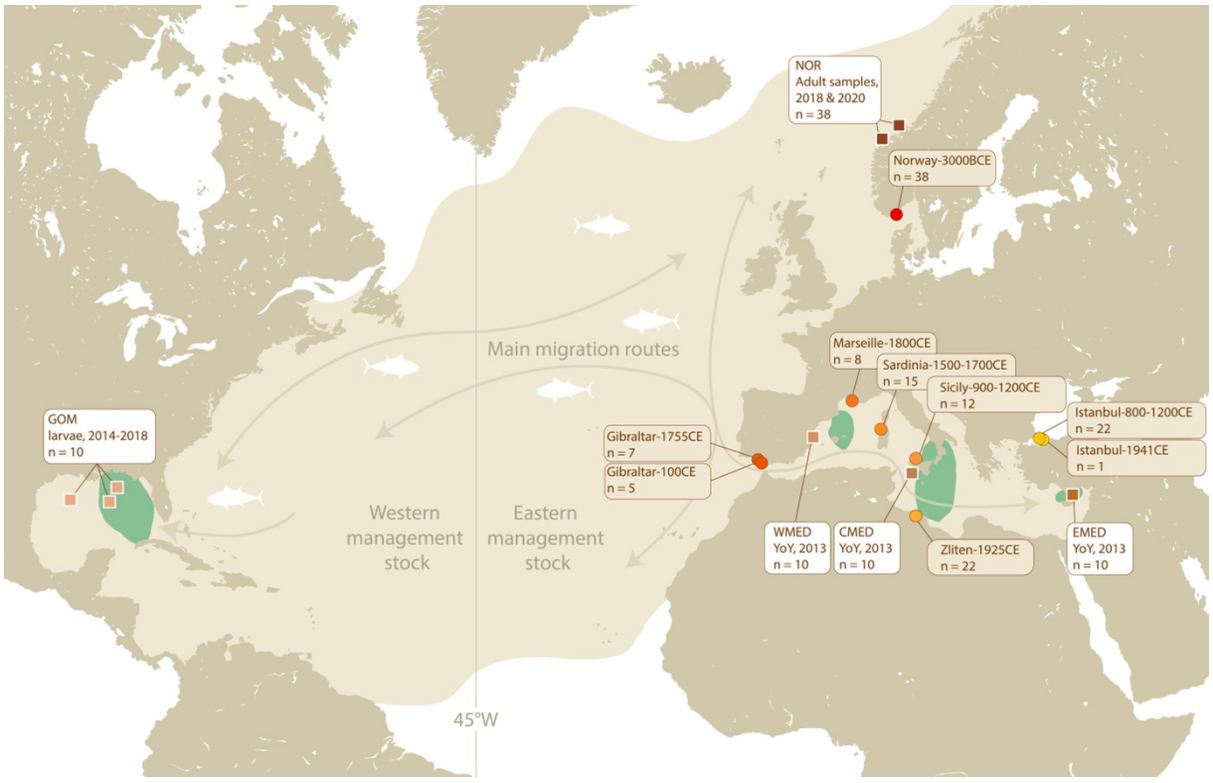

Figure 1: Distribution of the Atlantic bluefin tuna, including spawning areas (green) currently considered by management (adapted from IMR (2021)). The equal-distance line (45°W) separates the Eastern and Western stocks for management purposes. Sample locations of modern (squares, white boxes) and ancient tuna (circles, brown boxes) used in this study are indicated on the map. Arrows indicate the main migration routes of adult Atlantic bluefin (adapted from Fromentin et al., 2014). GOM = Gulf of Mexico, NOR = Norway, WMED = Western Mediterranean, CMED = Central Mediterranean, EMED = Eastern Mediterranean. YoY = young-of-the-year.

Methods

Collection, extraction, and sequencing of ancient samples from Norway

38 Neolithic (ca. 3000 BCE) tuna bones from the south of Norway were obtained from three archaeological excavations at Jortveit from 2018 to 2020. Bones were found at varying depths (42-130 cm) in six of nine total trenches and were estimated to be from 3700-2500 BCE based on radiocarbon dating of wood and charcoal from the sediment profiles, as well as directly dated bone harpoons. Three of the bones were also directly radiocarbon dated to the period approximately 3400-2800 BCE (Nielsen, 2020a, 2020b, 2020c; Nielsen & Persson, 2020).

All laboratory work prior to PCR was performed in a dedicated aDNA laboratory at the University of Oslo, following strict anti-contamination protocols (Gilbert et al., 2005; Llamas et al., 2017). Upon introduction to the aDNA lab, bones were brush-cleaned and UV-ed ten minutes on each side to reduce surface DNA contamination. The bones were then cut using an

electric dentistry tool with an attached cutting disc in a sterile extraction hood, preserving morphometric landmarks. Cut fragments were crushed using a custom designed stainless-steel mortar as described in Gondek, Boessenkool, and Star (2018).

All samples were extracted using a standard extraction protocol adapted from Dabney et al. (2013) after a pre-digestion step (DD from Damgaard et al. 2015) or mild bleach treatment and pre-digestion (BleDD from Boessenkool et al., 2017) as described in Ferrari et al. (2021) (Table S1). In summary, powdered bone (2 × 200 mg per sample) was subjected to the DD or BleDD treatment and digested in 1 ml 0.5 M EDTA, 0.5 mg/ml proteinase K and 0.5% N-Laurylsarcosine for 18-24 h at 37 C. Combined digests were extracted with 9 × volumes of PB buffer (QIAGEN) and DNA was purified with MinElute columns on a QIAvac 24 Plus vacuum manifold system (QIAGEN).

Dual-indexed sequencing libraries were built as double stranded, blunt-ended libraries following Meyer and Kircher (2010) and Kircher et al. (2012) with modifications or as single stranded libraries following the Santa Cruz Reaction (SCR) protocol (Kapp et al.2021) (Table S1). Meyer and Kircher libraries were built from 20 µL of ligated DNA extract or extraction blanks and performed in half volumes reactions. The single stranded SCR libraries were built from 3-20 µL of ligated DNA extract (depending on the DNA concentration) or 20 µL extraction blanks using dilution tier 4. Indexing PCRs were performed with Taq Pfu Turbo Cx HotStart DNA polymerase (Agilent) with the following cycling conditions: 2 min activation at 95 C, 30 s denaturation at 95 C, 30 s annealing at 60 C, 1 min elongation at 72 C, and 10 min final extension at 72 C. Sample extracts were subject to 12 PCR cycles, while extraction blanks were subject to 30 PCR cycles to increase the chance of detecting contamination. Amplified libraries were cleaned using Agencourt AMPure XP PCR purification beads (Bronner et al., 2013) and examined on a Fragment Analyzer™ (Advanced Analytical) using the High Sensitivity NGS Fragment Analysis Kit to determine suitability for sequencing. Libraries were sequenced on the Illumina HiSeq 4000 or NovaSeq 6000 (SP Flow Cell) platforms at the Norwegian Sequencing Centre with paired-end 150 bp reads and demultiplexed allowing zero mismatches in the index tag.

Ancient specimens from the Mediterranean

92 individuals from archaeological excavations and zoological collections throughout the Mediterranean region dating from 100 to 1941 CE were obtained from Andrews et al. (in prep.) as BAM files (Table S2). These samples were prepared and extracted in the Ancient DNA Laboratory of the Department of Cultural Heritage (University of Bologna, Ravenna Campus,

Italy), following strict criteria for aDNA analysis as per the Norwegian samples, and sequenced as single-stranded libraries (Kapp et al., 2021) at Macrogen facilities (Seoul, South Korea/Amsterdam, Netherlands) on a HiSeq X (100 bp paired-end) Illumina sequencing platform. Reads were processed using the Paleomix pipeline v.1.2.14 (Schubert et al., 2014) with settings described below (see "Bioinformatic processing of ancient and modern sequence data"), yielding an average of 28% endogenous DNA and 11-fold MT coverage (Table S8).

Collection, extraction, and sequencing of modern samples

Modern tuna tissue samples of migratory, foraging adults (total-weight range: 151 - 313 kg) from Norway (NOR) (n = 38) were collected by the Norwegian Institute of Marine Research (IMR), from commercial catch off the coast of Møre og Romsdal, Western Norway. Two batches of modern Norwegian samples were obtained, the first from September 2018 and the second from September 2020 (Table S3). These batches were taken from two single purse seine catches and each of them are therefore assumed to belong to the same shoal. The 2018 batch of samples was freeze dried muscle tissue powdered at IMR facilities. The 2020 batch was collected as skin samples cut out between the spines of the dorsal fin and submerged immediately in RNAlater, shipped, and placed in a -20°C freezer within a week. The modern samples from Norway were all extracted in the modern DNA isolation laboratories at the University of Oslo, using the DNeasy Blood & Tissue kit (Qiagen) and following the manufacturer's protocol.

Modern larvae or young-of-the-year (YoY) specimens (GOM: Gulf of Mexico, WMED: Western Mediterranean Balearic Islands, CMED: Central Mediterranean Sicily, EMED: Eastern Mediterranean Levantine Sea, n = 40, Table S4) were collected from each of the major Atlantic bluefin spawning sites (Figure 1) between 2013 and 2018. Juvenile albacore samples from the Bay of Biscay were caught by commercial vessels trolling in the Bay of Biscay between June and September of 2010 (Table S5). Larvae and tissue samples from each specimen were preserved in 96% ethanol and stored at -20 °C until further processing. Modern spawning site and albacore samples were extracted at the University of Bologna by a modified salt-based extraction protocol, as per Cruz et al. (2017), using SSTNE extraction buffer (Blanquer, 1990), and treated with RNase to remove residual RNA.

For all modern samples, DNA concentration was measured using a Qubit® dsDNA BR Assay Kit (Thermo Fisher Scientific, USA), where negative controls employed for each batch of samples extracted indicated undetectable levels of contamination. For the Norwegian samples, libraries were built using the TruSeq DNA Nano200 preparation kit (Illumina).

Modern spawning site extracts, along with albacore extracts, underwent single stranded library preparation following the SCR library protocol (Kapp et al., 2021). Sequencing and demultiplexing, allowing for zero mismatches, was performed at the Norwegian Sequencing Center on a combination of the HiSeq 4000 and NovaSeq 6000 (SP Flow Cell) Illumina sequencing platforms with paired-end 150 bp reads for all samples.

Raw sequence data of Pacific bluefin whole genome (Suda et al., 2019) were downloaded from DDBJ (accession no DRA008331) (Table S6) and used for interspecific population structure analyses.

Bioinformatic processing of ancient and modern sequence data

Both modern and ancient reads were processed using the Paleomix pipeline v.1.2.14 (Schubert et al., 2014). Adapters were removed and forward and reverse reads were collapsed and trimmed with AdapterRemoval v.2.3.1 (Schubert et al., 2016), discarding collapsed reads shorter than 25 bp. All reads were aligned to a draft nuclear (NCBI BioProject: PRJNA408269) and MT reference genome (GenBank accession nr NC_014052.1) with BWA-mem v.0.7.17 (Li & Durbin, 2009) for mapping. All reads were filtered to a minimum Phred score quality of 25, so that only reads with higher mapping quality to the reference genome were considered endogenous and used for subsequent analyses. PCR duplicates were removed in Picard Tools v.2.18.27 and indel realignment (*GATKs IndelRealigner*) was performed to produce final BAM files. DNA post-mortem damage patterns were assessed in mapDamage v.2.0.9 (Ginolhac et al., 2011; Jónsson et al., 2013) after downsampling to 100,000 randomly selected reads.

MT BAMfiles were further processed in GATK v.4.1.4.0 following GATK best practices (McKenna et al., 2010). Individual genotypes were called (GATK v.4.1.4.0 *HaplotypeCaller -ploidy 1*) and then combined into a joint gvcf (GATK v.4.1.4.0 *CombineGVCFs*) before genotyping (GATK v.4.1.4.0 *GenotypeGVCFs*). Genotypes were hard-filtered in BCFtools v.1.9 (Li et al., 2009) (*-i 'FS<60.0 && SOR<4 && MQ>30.0 && QD > 2.0' --SnpGap 10*) and VCFtools v.0.1.16 (Danecek et al., 2011) (*--minGQ 15 --minDP 2 --remove-indels*).

Filtered VCFs were indexed using Tabix v.0.2.6 (Li, 2011) and consensus sequences created as individual fasta files in BCFtools v.1.9 (bcftools consensus *-H 1*). Outgroup sequences were downloaded from GenBank (Clark et al., 2016) and curated using SeqKit v. 0.11.0 (*restart -i*) (Shen et al., 2016) so that all sequences started at position 1 in the D-loop, to correspond with the sample sequences. After renaming the fasta headers to their appropriate sample-IDs using BBMap v.38.50b (Bushnell, 2014) and combining the files to a multiple

sequence alignment (MSA), the joint fasta files were aligned using MAFFT v.7.453 (Katoh et al., 2002) (*--auto*).

Initial investigations and creation of datasets

Preliminary analyses were performed on a jointly called and filtered VCF and multiple-fasta, which included all samples. Missingness and depth was assessed for all samples using VCFtools v.0.1.16 (Danecek et al., 2011) and Principal Component analyses (PCA) (Adegenet (Jombart, 2008) in R v.4.1.2) and a Maximum Likelihood (ML) tree (IQTREE v. 1.6.12 (Nguyen et al., 2015), *-m MFP -bb 1000 -BIC*) was used to investigate clustering patterns and assess the presence of introgressed MT genomes. To look for identical haplotypes, we assessed the number of single nucleotide polymorphisms (SNPs) that differed between specimens using an in-house python3 script (https://github.com/laneatmore/nucleotide_differences), which uses MSAs as input to count the number of true SNP differences between all individuals (excluding those that were missing data) and generates distance matrices based on these differences.

Given that ancient bones may represent the same individual if they were obtained from the same archaeological context, we assessed the number of pairwise SNP differences between specimens at different filtering settings. To be conservative, ancient samples were considered identical if, in a pairwise comparison, they had no SNP differences at minDP2 *or* if they had only one SNP difference at minDP3 *and* came from the same archaeological layer. Using these criteria, we detected several genetically identical specimens of which the specimen with the highest endogenous DNA content was kept. Genetically identical modern samples were kept since distinct individuals were sampled. All samples with missingness above 50% (VCFtools v.0.1.16 *--missing-indv*, F_MISS) were also discarded. In total, 22 out of 208 samples (~10%) were discarded from further analyses (Table S7 and S8).

Datasets were created for each sampling location depending on the presence of introgressed MT genomes (Table S13). First, a dataset excluding the introgressed individuals was created to allow for comparison of the effect of introgressed haplotypes on summary statistics. A haplotype was assumed to be introgressed if it clustered with albacore or Pacific bluefin in the PCA (Figure S3). This clustering was additionally supported by the ML and BEAST trees, which revealed the same individuals falling into highly supported monophyletic clades with the respective species (Figure S4). As the genotyping and filtering process in the GATK pipeline is affected by the haplotype variants present in the analyses, only samples within each dataset should be called and filtered together to accurately present the variation (GATK, 2016). These separate datasets were therefore separately genotyped, filtered, and

aligned (with settings described in the section above) to create respective multiple-fasta files for subsequent analyses. An overview of these individual datasets can be found in Table S14.

Population genomic analyses

Genetic population structure was investigated using Principal Component analyses (PCA) as implemented in the R-package Adegenet (Jombart, 2008). A map of missing loci and alleles diverging from the reference genome, was created to assess missing genotypes in both ancient and modern samples and better visualize introgressed specimens. All plots were created with R 4.3 in RStudio (Rstudio Team 2021), using various packages for data loading, analyses, and visualization (see supplementary Section 1).

Genetic diversity was investigated using a range of standard population genetic measurements. The number of haplotypes (Nh) and haplotype diversity (hD) (Nei 1987) was calculated in R-package pegas (Paradis, 2010) and independently assessed in Fitchi (Matschiner, 2016). The number of segregating sites (S), nucleotide diversity (π) (Nei 1987), Tajima's D (TD) (Tajima, 1989), and Fu and Li's F statistic (F) (Fu & Li, 1993) were calculated in DnaSP v.6 (Rozas et al., 2017).S, π, TD values were confirmed in pegas. To account for differences in sample sizes across sites when calculating π and TD, an additional analysis using 1000 bootstrap replicates and subsampling five individuals per round without replacement, was performed in pegas on datasets where the total sample size was over five.

Phylogenetic relationships were investigated using both ML and Bayesian approaches. ML trees with 100 nonparametric bootstrap replicates were created in IQTREE v. 1.6.12 (Nguyen et al., 2015). ModelFinder Plus (MFP) (Kalyaanamoorthy et al., 2017) was used to search all available models, and best-fit models were selected according to the Bayesian Information Criterion (BIC) (Schwarz, 1978). Bayesian trees were created in BEAST 2 v.2.6.4 (R. Bouckaert et al., 2014), using the Yule model prior under a strict clock with mutation rate 3.6×10^{-8} substitutions per site per year as per Donaldson and Wilson (1999), running MCMC over 800,000,000 generations and sampling once every 1000 generations. bModelTest (R. R. Bouckaert & Drummond, 2017) was used to assess available site models, and the resulting logfile was inspected in Tracer v1.7.2 (Rambaut et al., 2018). Trees were downsampled in LogCombiner (implemented in BEAST 2 v.2.6.4), resampling every 10,000 trees. TreeAnnotator (implemented in BEAST 2 v.2.6.4) was used to remove the first 10% of the trees (burnin) and create a target maximum clade credibility tree. Nodes with less than 50% posterior support were excluded from the summary analysis in TreeAnnotator so that only

nodes present in the majority of the trees were annotated. The final trees in all phylogenetic analyses were visualized and curated in FigTree v.1.4.4 (Rambaut, 2018).

Evolutionary relationships were visualized using haplotype networks created in Fitchi (*--haploid -p*) (Matschiner, 2016) using the ML trees generated in IQTREE (described above) as input with bootstrap values removed using the R-package ape (Paradis et al., 2004). For the dataset including introgressed individuals and outgroup species, a minimum edge length of seven substitutions was defined (*-e 7*) so that haplotypes separated by seven or fewer substitutions were collapsed into one node. For the dataset only containing Atlantic bluefin haplotypes, each node was defined as a unique haplotype (*-e 1*).

Genetic distance between sample locations was assessed using measures of absolute (d_{xy}) and relative (ΦST) divergence, calculated using DnaSP v.6 ("*DNA divergence between populations", all sites*) (Rozas et al., 2017) and Arlequin v.3.5 (Excoffier & Lischer, 2010) respectively. In Arlequin, pairwise ΦST was calculated via a distance matrix computed by Arlequin based on Tamura & Nei (1993) and assuming no rate heterogeneity, as suggested by bModelTest (R. R. Bouckaert & Drummond, 2017) (implemented in BEAST 2 v.2.6.4 (R. Bouckaert et al., 2014)). To test the significance of ΦST, p-values were generated in Arlequin using 1000 permutations.

Results

DNA yield and library success

A total of 1.7 billion sequencing reads were obtained for the 38 ancient samples from Norway. These specimens had remarkable DNA preservation with 100% library success and yielding, on average, 24% endogenous DNA and 20-fold MT coverage (Table S7). The reads showed postmortem degradation patterns expected for authentic ancient DNA (Figure S2). A total of 3.1 billion sequencing reads were obtained for the 84 modern specimens, resulting in 711-fold MT coverage on average for the 78 Atlantic bluefin specimens (Table S9 and S10) and 221-fold MT coverage on average for the six albacore samples (Table S11). The Pacific bluefin raw sequence data from Suda et al. (2019) yielded 3322-fold MT coverage (Table S12). After stringent filtering, 186 out of 208 specimens (~90%) were kept for further analyses (Table S7 and S8).

Detecting introgressed MT mitogenomes

Out of 186 samples analyzed, seven ancient and four modern individuals had MT haplotypes that clustered closely with albacore or Pacific bluefin in both the PCA, haplotype network and

phylogenies. The PCA reveals three distinct clusters (Figure 2) with PC1 separating an Atlantic bluefin cluster from a Pacific bluefin and albacore cluster and PC2 separating the latter two speciese. Within the Pacific bluefin cluster, we observe two modern (both NOR) and four ancient (two Norway 3000BCE, one Istanbul 800-1200CE and one Sardinia 1500-1700CE) Atlantic bluefin specimens. Within the albacore cluster, we observe two modern (one NOR and one WMED) and three ancient (one Istanbul-800-1200CE and two Sicily-900-1200CE) Atlantic bluefin specimens. The PCA-clusters are reiterated in the haplotype network (Figure 2). ML and Bayesian phylogenetic analyses provided full statistical support (bootstrap=100, posterior probability=1) for the three species as monophyletic groups with the same six Pacific-like and five albacore-like haplotypes again clustering with their respective species (Figure 2, see also Figure S6). We conclude that these Pacific-like and albacore-like haplotypes are introgressed MT genomes into Atlantic bluefin tuna.

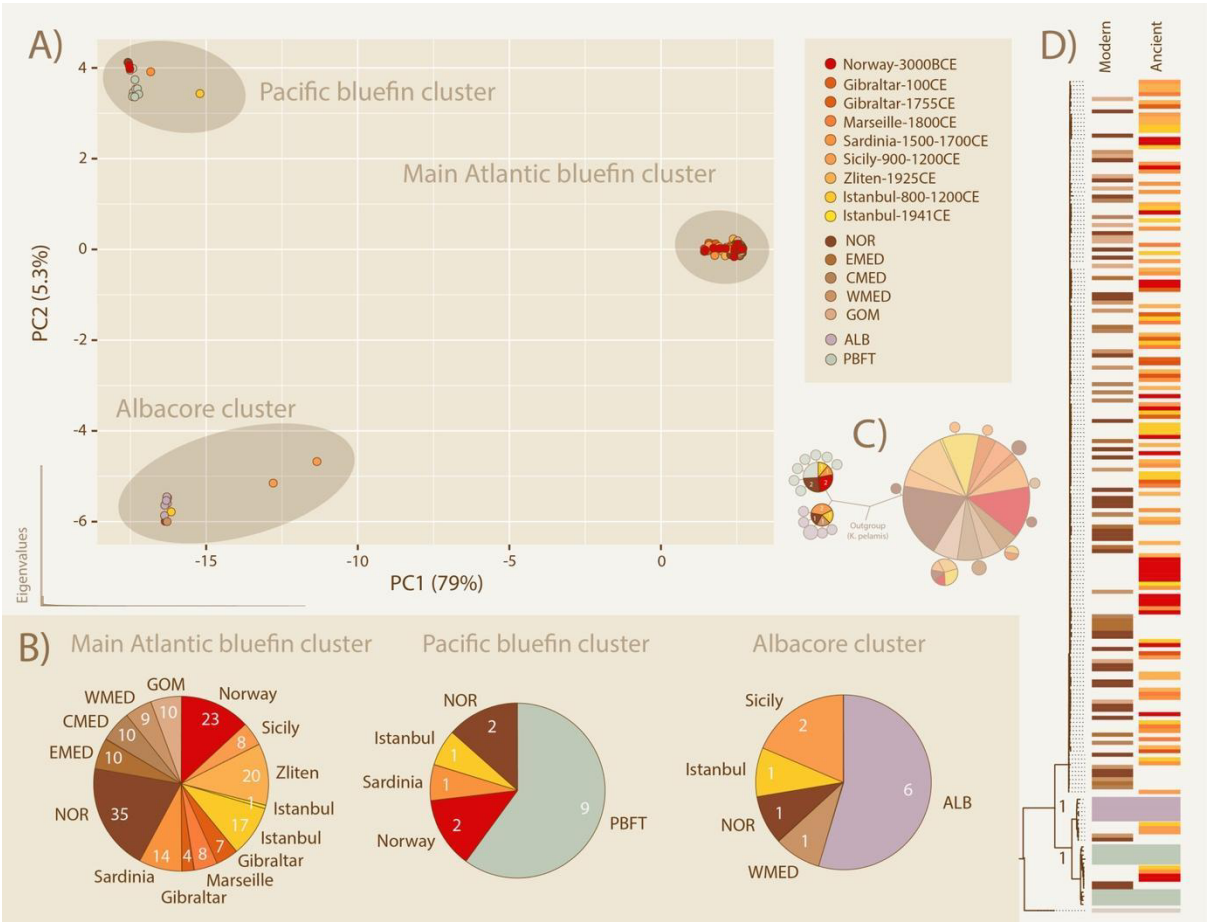

Figure 2: Species clusters and introgressed MT haplotypes within Atlantic bluefin specimens, revealed by PCA, haplotype network and phylogenetic analyses A) Three species specific clusters detected in ancient and modern Atlantic tuna specimens. The PCA shows three species specific clusters and PCA eigenvalues are shown in the bottom left corner. Modern modern Pacific tuna (blue) and albacore (grey) specimens are included as controls. B) Relative abundance of haplotypes per location within each PCA-cluster is visualized as pie-charts, with the number of samples from each location indicated on the slices. C) Haplotype network showing three species specific haplotypes. Haplotypes separated by seven or fewer substitutions were collapsed into single nodes. D)

Interspecific phylogeny of specimens with posterior probability support for the species clades (see also Figure S6). Colors are representative of the spatiotemporal cohorts listed in the legend of panel A).

Spatiotemporal population structure

We find no significant genomic differentiation between any of the temporal cohorts. We also observe no spatial differences in the level of genetic variation between any of the sampling locations for Atlantic bluefin. Atlantic bluefin individuals from both management stocks and across the Eastern stock range and spawning areas are scattered across the intraspecific PCA (Figure S8) and haplotype network (Figure S9). The sampling locations are also distributed along the entire phylogeny within the Atlantic bluefin group (Figure 2, see also Figure S6 and S10). The intraspecific Atlantic bluefin haplotype network reveals a star-like pattern with more recent haplotypes deriving from an ancestral, central haplotype (Figure S9).

Genetic divergence and diversity influenced by introgression

Measures of pairwise genetic distance between Atlantic bluefin sampling locations show low levels of absolute (d_{xy}) and relative (Φst) divergence, either excluding (Figure 3a) or including introgressed MT haplotypes (Figure 3b). Genetic differentiation increases when introgressed samples are included. This increase is driven by the inclusion of genetically more divergent haplotypes, which are not present at each location or temporal cohort. In all cases, levels of Φst remained low and non-significant (Figure S7) across all populations. Including individuals with introgressed MT haplotypes increased values of nucleotide diversity π and S (Table S15). The number of haplotypes (hD) is not impacted; most sample locations only contained unique specimens (N=Nh) therefore leading to a hD of 1, meaning 100% probability of obtaining unique samples during random sampling. Tajima's D (TD) was also not affected by the inclusion of introgressed individuals and was significantly negative for most locations and temporal cohorts and when analyzing all specimens jointly (Table S15).

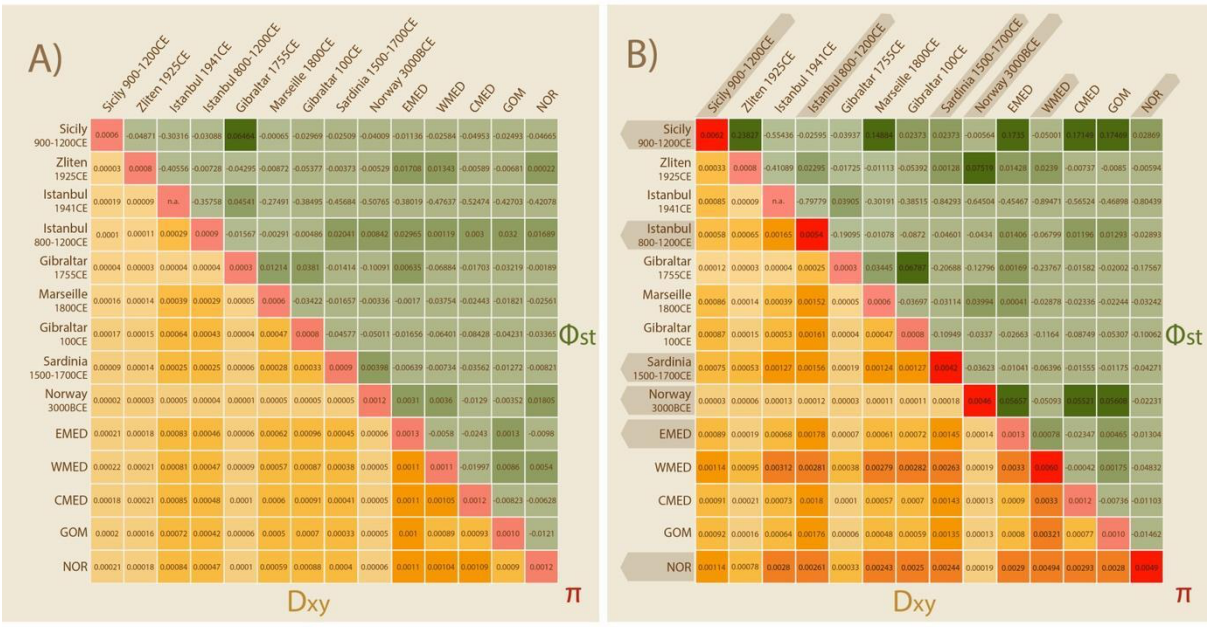

Figure 3: No significant spatiotemporal population structure in Atlantic bluefin tuna based on mitogenomic data of 186 specimens. Pairwise population divergence is presented as a heatmap showing absolute (d_{xy}) and relative (ΦST) divergence between populations when A) excluding and B) including the introgressed mitogenomes. Divergence is inflated when including introgressed mitogenomes. Locations containing introgressed individuals are highlighted with darker shading in panel B). The nucleotide diversity within each population is shown on the diagonal. P-values for ΦST can be found in supplementary (Figure S7).

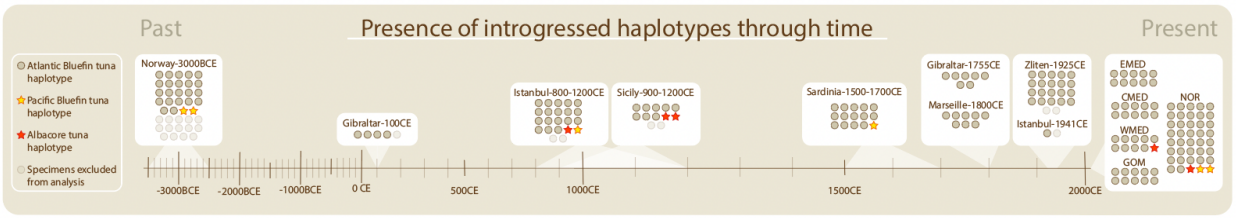

Figure 4: Introgressed Pacific bluefin MT haplotypes (yellow stars) or albacore MT haplotypes (red stars) are observed along an entire 5000-year-old chronology of ancient Atlantic bluefin tuna specimens. Individual tuna specimens (n=208) (circle or star) are grouped according to their age, determined by archaeological context. Specimens were either modern (n=78), or ancient (n=130) and dated by archaeological context. Uncertainty in the age range of ancient specimens is depicted beneath their respective sample sets (light shading).

MT haplotype introgression over time

We observe MT haplotype introgression into Atlantic bluefin throughout a 5000-year chronology (Figure 4). The earliest observation is the presence of two introgressed MT haplotypes from Pacific bluefin in the Neolithic (ca. 3000 BCE) in Norway. Pacific bluefin tuna MT haplotypes are further found in early medieval Istanbul (800-1200CE), late-medieval Sardinia (1500-1700 CE) and modern Norway. Albacore MT haplotypes are found in early medieval Istanbul (800-1200CE) and Sicily (900-1200CE), modern Western Mediterranean and modern Norway.

Discussion

We here present a 5000-year chronology of MT introgression in the Atlantic bluefin tuna. The presence of introgressed MT haplotypes in the Neolithic (ca. 3000 BCE), turn of the millennium (800-1200 CE), and in present day populations reveals that introgression resulted from long-term natural phenomena rather than being a consequence of recent anthropogenic impacts. Moreover, our results show that the frequency of introgression in the Atlantic bluefin has remained stable over millennia despite shifts in abundance and distribution of Atlantic bluefin populations.

Evidence of mitochondrial introgression through time

We obtain similar rates of MT introgression as reported by previous studies in our modern samples, with rates of introgression for Pacific bluefin and albacore at 2.6% (2/78 individuals) each. Including our ancient samples in the calculation, the rate of introgression remains astonishingly stable with 3.2% Pacific bluefin haplotypes (6/186) and 2.7% albacore-like haplotypes (5/186) across all samples. In total, six Pacific-like and five albacore-like haplotypes consistently cluster with their respective species through all interspecific analyses. We do not observe albacore-like haplotypes from the Neolithic period, but because of the low frequency of introgression compared to the sample size we speculate this is likely due to sampling stochasticity rather than lack of natural hybridization at the time. Still, it cannot be excluded that Neolithic climate conditions drove albacore populations away from areas inhabited by Atlantic bluefin.

The location of the hybridization events with introgressive hybridization from both albacore and Pacific bluefin remain to be investigated. While the albacore has overlapping ranges and spawning areas with both bluefin species, the Pacific and Atlantic bluefins are geographically separated with no documented migration. The potential migration of Pacific bluefin into the Atlantic Ocean has been hypothesized to occur via the Indian Ocean and following the Agulhas current around the tip of Africa (Bremer et al. 2005). Whether this represents a contemporary migration route or a historical process where past, stronger currents might have facilitated admixture is unclear (Bremer et al. 2005). The similar rate of introgression from both albacore and Pacific bluefin and the lack of introgressed MT haplotypes in the albacore makes the range-overlapping albacore an unlikely carrier of MT haplotypes between the bluefins. As Pacific bluefin also contains Atlantic bluefin-like MT haplotypes, another hypothesis for their presence is incomplete lineage sorting (ILS). The Thunnus genus is thought to have diverged rapidly within the last 6-10 million years, with a

more recent speciation of the Pacific and Atlantic bluefins only around 400,000 years ago (Santini et al. 2013; Ciezarek et al. 2018; Díaz-Arce et al. 2016). While introgressive hybridization is the likely origin of albacore-like haplotypes in both bluefin species (Ciezarek et al. 2018), observed gene-tree versus species-tree discordance that did not deviate from expectations under ILS. These results indicate that the observed patterns of Pacific-like MT haplotypes in the Atlantic bluefin population, and vice versa, may be a result of ILS rather than introgressive hybridization. Larger genomic databases are required to furhter delineate between these two hypotheses.

While our historical investigation focuses on the eastern Atlantic with samples from the Mediterranean and Norway, introgressed MT genomes from albacore have also been found in the Gulf of Mexico (1% frequency) and the Slope Sea (6% frequency). Because introgressed MT genomes in Atlantic bluefin were first observed in the eastern Atlantic, their presence in the western Atlantic has been hypothesized to be introduced via gene flow from the Mediterranean (Diaz-Arce et al., 2024). An increase in gene flow from the Mediterranean into the Gulf of Mexico and Slope Sea will likely erode genetic differences between the two management stocks (Diaz-Arce et al., 2024). Direct observations of intogression events within the Western Atlantic bluefin stock have not been made, although albacore is known to spawn across tropical waters including the South-West Sargasso Sea as well as the Mediterranean (ICCAT, 2016, 2020; NOAA, 2023). Future studies should investigate long-term MT introgression in the Gulf of Mexico to disentangle the recently suggested changes in demographic patterns (Diaz-Arce et al., 2024) and locate the origins of the intogression events.

Introgressed haplotypes impact estimates of genomic differentiation

We observe that the presence of introgressed haplotypes increases measures of genetic diversity (S and π), which is driven by the highly divergent alleles of such introgressed MT genomes (Figure S5). The inclusion of these diverging haplotypes also influences the measures of genetic divergence (d_{xy} and ΦST) between locations and temporal cohorts, consistently increasing the absolute genetic diversity (d_{xy}) and altering the pattern of relative genetic divergence (ΦST). Tajima's D (TD) was not consistently affected by the inclusion of introgressed individuals, although in some cases TD changed value and lost or attained significance when introgressed haplotypes were included (Table S15). Considering these results, it is important to be aware of highly diverging haplotypes when extrapolating population genetic statistics from subsamples of natural populations containing highly diverging haplotypes. The low frequency of natural hybridization in Atlantic bluefin causes

stochasticity at low sample sizes, and we find that the inclusion of introgressed individuals inflates population genomic statistics that are commonly used for management and population viability assessments (Hohenlohe et al., 2021).

Spatiotemporal population structure

We find no significant divergence and no pattern of genomic MT differentiation between any of the spatial or temporal cohorts. Ancient and modern samples largely intermixed in all analyses, suggesting mitogenomic stability and temporal continuity through time. Similar observations in other species, such as Atlantic cod (*Gadus morhua*) (Martínez-García et al., 2021) and New Zealand snapper (*Chrysophrys auratus*) (Oosting et al., 2023) emphasize the low power of the MT genome to observe spatiotemporal differentiation in wide ranging fish species. The regular presence of identical haplotypes across sampling locations and temporal cohorts emphasizes the lack of mitogenomic variation and informative markers for population structure in this species. Although we cautiously removed identical samples from the same archaeological excavations, the presence of identical samples across cohorts that were processed in different laboratories shows this as a naturally occurring phenomenon.

Population genetic statistics confirmed low mitogenomic variation with no significant divergence between any of the spatiotemporal cohorts and no temporal loss of genetic diversity despite heavy exploitation (Figure 3A, Table S15). Across datasets, TD was negative and often significant, suggesting an excess of rare alleles in the datasets. This is indicative of either positive selection or recent population expansion (Fijarczyk & Babik, 2015; Delph & Kelly, 2014). Population expansion is further corroborated in the intraspecific haplotype network, where newer haplotypes are derived from a shared central haplotype forming a star-like pattern (Figure S9). These results highlight robust preservation of the MT genome despite centuries of human exploitation.

Conclusion

Atlantic bluefin tuna has experienced significant changes in distribution linked to sea surface temperature oscillations during the past centuries (Faillettaz et al., 2019; Muhling et al., 2011; Ravier & Fromentin, 2004), alongside intense exploitation (Andrews et al., 2022; Block, 2019), biomass depletion, range contraction, trophic niche loss (Andrews et al., 2023; Di Natale, 2015; Tangen, 2009), followed by recovery, increased biomass, and range expansion of the Eastern Atlantic bluefin stock during the last decade (Nøttestad et al. 2020; ICCAT 2023). Despite such

extensive spatial shifts in distribution over time, we show that MT introgression is a long-term natural phenomenon in Atlantic bluefin. The stable frequency over time suggests that this phenomenon is robust against historical climate fluctuations and more recent anthropogenic impacts. By providing a baseline observation, our study highlight the utility of ancient DNA to obtain temporal insights in the long-term persistence of such phenomena, which is essential for disentangling the drivers of introgression and any fitness consequences of MT intogression.

Acknowledgements

This work was supported by the European Union's Horizon 2020 Research and Innovation Programme under the Marie Skłodowska-Curie grant agreement No. 813383 (SeaChanges) and the 4-OCEANS Synergy grant agreement no. 951649. The European Research Agency is not responsible for any use that may be made of the information this work contains. Special thanks goes to the Norwegian Sequencing Centre (University of Oslo; https://www.sequencing.uio.no) for the sequencing of genomic libraries. Computation was performed using the resources and assistance from SIGMA2. The collection of recent samples in Norway was financed by the Institute of Marine Research. The collection of larva samples in the Gulf of Mexico was funded by the NOAA RESTORE Science Program, BLOOFINZ-GoM #NOAA-NOS-NCCOS-2017-2004875; Cooperative Institute for Marine and Atmospheric Studies #NA20OAR4320472. This work is a contribution to the https://tunaarchaeology.org/ project.

We are grateful to Ørjan Sørensen at the Institute of Marine Research (IMR) for his contributions to the collection and shipping of the modern Atlantic bluefin samples from Norway and providing sample metadata. We thank Verónica Gómez-Fernández (Instituto Nacional de Investigaciones Científicas y Ecológicas, Spain), Gabriele Carenti (CEPAM, CNRS, Université Côte d'Azur, France) and Darío Bernal-Casasola (Department of History, Geography and Philosophy, Faculty of Philosophy and Letters, University of Cádiz, Spain) for sample collection. We thank Leif Nøttestad (IMR) and Mark Ravinet (CEES, University of Oslo) for comments and stimulating scientific discussions.

Author contributions following CRediT (https://credit.niso.org/)

Emma Falkeid Eriksen: Conceptualization, Data curation, Formal Analysis, Investigation, Methodology, Visualization, Writing – original draft, Writing – review & editing

Adam Jon Andrews: Data curation, Investigation, Methodology, Writing – review & editing

Svein Vatsvåg Nielsen: Resources, Writing – review & editing

Per Persson: Writing – review & editing

Estrella Malca: Resources, Writing – review & editing

Vedat Onar: Resources

Veronica Aniceti: Resources

Gäel Piquès: Resources

Federica Piattoni: Data curation, methodology, Writing – review & editing

Francesco Fontani: Investigation

Martin Wiech: Resources, Writing-review & editing

Keno Ferter: Resources, Writing-review & editing

Oliver Kersten: Investigation, Writing-review & editing

Giada Ferrari: Investigation, Writing-review & editing

Alessia Cariani: Resources, Funding acquisition, Writing-review & editing

Fausto Tinti: Resources, Funding acquisition, Writing-review & editing

Elisabetta Cilli: Resources, Funding acquisition

Lane M. Atmore: Software, Supervision, Writing – review & editing

Bastiaan Star: Conceptualization, Funding acquisition, Project administration, Software, Supervision, Writing – original draft, Writing – review & editing

Competing interests

The authors declare no competing interests.

Data archiving

All mitochondrial BAM files used in this study has been uploaded in the European Nucleotide Archive (ENA) and can be accessed at https://www.ebi.ac.uk/ena/browser/view/PRJEB74135. See supplementary csv containing filenames, project accession number and ENA identifier for all samples.

References

A.J. Andrews, B. Star, A. Di Natale, E. Malca, G. Zapfe, D. Bernal-Casasola, V. Onar, V. Aniceti, G. Carenti, G. Piques, F. Piattoni, F. Fontani, E.F. Eriksen, L. Atmore, O. Kersten, F. Tinti, E. Cilli, A. Cariani. One millennia of nuclear genomes reveal the demographic history of Atlantic bluefin tuna. In prep.

Aalto, E. A., Dedman, S., Stokesbury, M. J. W., Schallert, R. J., Castleton, M., & Block, B. A. (2023). Evidence of bluefin tuna (*Thunnus thynnus*) spawning in the Slope Sea region of the Northwest Atlantic from electronic tags. *ICES Journal of Marine Science*, *80*(4), 861–877. https://doi.org/10.1093/icesjms/fsad015

Alvarado Bremer, J. R., Naseri, I., & Ely, B. (1997). Orthodox and unorthodox phylogenetic relationships among tunas revealed by the nucleotide sequence analysis of the mitochondrial DNA control region. *Journal of Fish Biology*, 50(3), 540–554. https://doi.org/10.1111/j.1095-8649.1997.tb01948.x

Alvarado Bremer, J. R., Viñas, J., Mejuto, J., Ely, B., & Pla, C. (2005). Comparative phylogeography of Atlantic bluefin tuna and swordfish: The combined effects of vicariance, secondary contact, introgression, and

population expansion on the regional phylogenies of two highly migratory pelagic fishes. *Molecular Phylogenetics and Evolution*, *36*(1), 169–187. https://doi.org/10.1016/j.ympev.2004.12.011

Andrews, A. J., Di Natale, A., Bernal-Casasola, D., Aniceti, V., Onar, V., Oueslati, T., Theodropoulou, T., Morales-Muñiz, A., Cilli, E., & Tinti, F. (2022). Exploitation history of Atlantic bluefin tuna in the Eastern Atlantic and Mediterranean—Insights from ancient bones. *ICES Journal of Marine Science*, *79*(2), 247–262. https://doi.org/10.1093/icesjms/fsab261

Andrews, A. J., Pampoulie, C., Di Natale, A., Addis, P., Bernal-Casasola, D., Aniceti, V., Carenti, G., Gómez-Fernández, V., Chosson, V., Ughi, A., Von Tersch, M., Fontanals-Coll, M., Cilli, E., Onar, V., Tinti, F., & Alexander, M. (2023a). Exploitation shifted trophic ecology and habitat preferences of Mediterranean and Black Sea bluefin tuna over centuries. *Fish and Fisheries*. https://doi.org/10.1111/faf.12785

Andrews, A. J., Orton, D., Onar, V., Addis, P., Tinti, F., & Alexander, M. (2023b). Isotopic life-history signatures are retained in modern and ancient Atlantic bluefin tuna vertebrae. *Journal of Fish Biology*, 103(1), 118–129. https://doi.org/10.1111/jfb.15417

Andrews, A. J., Puncher, G. N., Bernal-Casasola, D., Di Natale, A., Massari, F., Onar, V., Toker, N. Y., Hanke, A., Pavey, S. A., Savojardo, C., Martelli, P. L., Casadio, R., Cilli, E., Morales-Muñiz, A., Mantovani, B., Tinti, F., & Cariani, A. (2021). Ancient DNA SNP-panel data suggests stability in bluefin tuna genetic diversity despite centuries of fluctuating catches in the eastern Atlantic and Mediterranean. *Scientific Reports*, *11*(1), 20744. https://doi.org/10.1038/s41598-021-99708-9

Atmore, L. M., Ferrari, G., Martínez-García, L., van der Jagt, I., Blevis, R., Granado, J., Häberle, S., Dierickx, K., Quinlan, L. M., Lõugas, L., Makowiecki, D., Hufthammer, A. K., Barrett, J. H., & Star, B. (2023). Ancient DNA sequence quality is independent of fish bone weight. Journal of Archaeological Science, 149, 105703. https://doi.org/10.1016/j.jas.2022.105703

Ballard, J. W. O., & Whitlock, M. C. (2004). The incomplete natural history of mitochondria. *Molecular Ecology*, *13*(4), 729–744. https://doi.org/10.1046/j.1365-294X.2003.02063.x

Benestan, L. M., Rougemont, Q., Senay, C., Normandeau, E., Parent, E., Rideout, R., Bernatchez, L., Lambert, Y., Audet, C., & Parent, G. J. (2021). Population genomics and history of speciation reveal fishery management gaps in two related redfish species (*Sebastes mentella* and *Sebastes fasciatus*). *Evolutionary Applications*, *14*(2), 588–606. https://doi.org/10.1111/eva.13143

Blanquer, A. (1990). Phylogéographie intraspécifique d'un poisson marin, le flet *Platichthys flesus* L. (Heterosomata): Polymorphisme des marqueurs nucléaires et mitochondriaux [Thesis, Montpellier 2]. In *Http://www.theses.fr*. http://www.theses.fr/1990MON20015

Block, B. A. (2019). *The Future of Bluefin Tunas: Ecology, Fisheries Management, and Conservation*. JHU Press.

Block, B. A., Teo, S. L. H., Walli, A., Boustany, A., Stokesbury, M. J. W., Farwell, C. J., Weng, K. C., Dewar, H., & Williams, T. D. (2005). Electronic tagging and population structure of Atlantic bluefin tuna. *Nature*, *434*(7037), 1121–1127. https://doi.org/10.1038/nature03463

Boessenkool, S., Hanghøj, K., Nistelberger, H. M., Der Sarkissian, C., Gondek, A. T., Orlando, L., Barrett, J. H., & Star, B. (2017). Combining bleach and mild predigestion improves ancient DNA recovery from bones. *Molecular Ecology Resources*, *17*(4), 742–751. https://doi.org/10.1111/1755-0998.12623

Bouckaert, R., Heled, J., Kühnert, D., Vaughan, T., Wu, C.-H., Xie, D., Suchard, M. A., Rambaut, A., & Drummond, A. J. (2014). BEAST 2: A Software Platform for Bayesian Evolutionary Analysis. *PLOS Computational Biology*, *10*(4), e1003537. https://doi.org/10.1371/journal.pcbi.1003537

Bouckaert, R. R., & Drummond, A. J. (2017). bModelTest: Bayesian phylogenetic site model averaging and model comparison. *BMC Evolutionary Biology*, *17*(1), 42. https://doi.org/10.1186/s12862-017-0890-6

Boustany, A. M., Reeb, C. A., & Block, B. A. (2008). Mitochondrial DNA and electronic tracking reveal population structure of Atlantic bluefin tuna (*Thunnus thynnus*). *Marine Biology*, *156*(1), 13–24. https://doi.org/10.1007/s00227-008-1058-0

Brauer, C. J., Sandoval-Castillo, J., Gates, K., Hammer, M. P., Unmack, P. J., Bernatchez, L., & Beheregaray, L. B. (2023). Natural hybridization reduces vulnerability to climate change. *Nature Climate Change*, *13*(3), Article 3. https://doi.org/10.1038/s41558-022-01585-1

Bronner, I. F., Quail, M. A., Turner, D. J., & Swerdlow, H. (2013). Improved Protocols for Illumina Sequencing. *Current Protocols in Human Genetics*, *79*(1), 18.2.1-18.2.42. https://doi.org/10.1002/0471142905.hg1802s79

Brophy, D., Haynes, P., Arrizabalaga, H., Fraile, I., Fromentin, J. M., Garibaldi, F., Katavic, I., Tinti, F., Karakulak, F. S., Macías, D., Busawon, D., Hanke, A., Kimoto, A., Sakai, O., Deguara, S., Abid, N., & Santos, M. N. (2016). Otolith shape variation provides a marker of stock origin for north Atlantic bluefin tuna (*Thunnus thynnus*). *Marine and Freshwater Research*, *67*(7), 1023–1036. https://doi.org/10.1071/MF15086

Brown, K. H. (2008). Fish mitochondrial genomics: Sequence, inheritance and functional variation. *Journal of Fish Biology*, *72*(2), 355–374. https://doi.org/10.1111/j.1095-8649.2007.01690.x

Bushnell, B. (2014). *BBMap: A Fast, Accurate, Splice-Aware Aligner* (LBNL-7065E). Lawrence Berkeley National Lab. (LBNL), Berkeley, CA (United States). https://www.osti.gov/biblio/1241166

Carlsson, J., McDOWELL, J. R., Díaz-Jaimes, P., Carlsson, J. E. L., Boles, S. B., Gold, J. R., & Graves, J. E. (2004). Microsatellite and mitochondrial DNA analyses of Atlantic bluefin tuna (*Thunnus thynnus thynnus*) population structure in the Mediterranean Sea. *Molecular Ecology*, *13*(11), 3345–3356. https://doi.org/10.1111/j.1365-294X.2004.02336.x

Cayuela, H., Rougemont, Q., Laporte, M., Mérot, C., Normandeau, E., Dorant, Y., Tørresen, O. K., Hoff, S. N. K., Jentoft, S., Sirois, P., Castonguay, M., Jansen, T., Praebel, K., Clément, M., & Bernatchez, L. (2020). Shared ancestral polymorphisms and chromosomal rearrangements as potential drivers of local adaptation in a marine fish. *Molecular Ecology*, *29*(13), 2379–2398. https://doi.org/10.1111/mec.15499

Chow, S., & Inoue, S. (1993). *Intra and interspesific restriction fragment length polymorphism in mitochondrial genes of Thunnus tuna species*.

Chow, S., & Kishino, H. (1995). Phylogenetic relationships between tuna species of the genus Thunnus (Scombridae: Teleostei): Inconsistent implications from morphology, nuclear and mitochondrial genomes. *Journal of Molecular Evolution*, *41*(6). https://doi.org/10.1007/BF00173154

Chow, S., Nakagawa, T., Suzuki, N., Takeyama, H., & Matsunaga, T. (2006). Phylogenetic relationships among Thunnus species inferred from rDNA ITS1 sequence. *Journal of Fish Biology*, *68*(A), 24–35. https://doi.org/10.1111/j.0022-1112.2006.00945.x

Chow, S., & Ushiama, H. (1995). Global population structure of albacore (Thunnus alalunga) inferred by RFLP analysis of the mitochondrial ATPase gene. *Marine Biology*, *123*(1), 39–45. https://doi.org/10.1007/BF00350321

Ciezarek, A. G., Osborne, O. G., Shipley, O. N., Brooks, E. J., Tracey, S. R., McAllister, J. D., Gardner, L. D., Sternberg, M. J. E., Block, B., & Savolainen, V. (2019). Phylotranscriptomic Insights into the Diversification of Endothermic Thunnus Tunas. Molecular Biology and Evolution, 36(1), 84–96. https://doi.org/10.1093/molbev/msy198

Clark, K., Karsch-Mizrachi, I., Lipman, D. J., Ostell, J., & Sayers, E. W. (2016). GenBank. *Nucleic Acids Research*, *44*(Database issue), D67–D72. https://doi.org/10.1093/nar/gkv1276

Colbeck, G. J., Turgeon, J., Sirois, P., & Dodson, J. J. (2011). Historical introgression and the role of selective vs. Neutral processes in structuring nuclear genetic variation (AFLP) in a circumpolar marine fish, the capelin (Mallotus villosus). *Molecular Ecology*, *20*(9), 1976–1987. https://doi.org/10.1111/j.1365-294X.2011.05069.x

Collette, B. B., Reeb, C., & Block, B. A. (2001). Systematics of the tunas and mackerels (Scombridae). *Fish Physiology* (Vol. 19, pp. 1–33). Academic Press. https://doi.org/10.1016/S1546-5098(01)19002-3

Cruz, V. P., Vera, M., Pardo, B. G., Taggart, J., Martinez, P., Oliveira, C., & Foresti, F. (2017). Identification and validation of single nucleotide polymorphisms as tools to detect hybridization and population structure in freshwater stingrays. *Molecular Ecology Resources*, *17*(3), 550–556. https://doi.org/10.1111/1755-0998.12564

Dabney, J., Knapp, M., Glocke, I., Gansauge, M.-T., Weihmann, A., Nickel, B., Valdiosera, C., Garcia, N., Paabo, S., Arsuaga, J.-L., & Meyer, M. (2013). Complete mitochondrial genome sequence of a Middle Pleistocene cave bear reconstructed from ultrashort DNA fragments. *Proceedings of the National Academy of Sciences*, *110*(39), 15758–15763. https://doi.org/10.1073/pnas.1314445110

Dagilis, A. J., Peede, D., Coughlan, J. M., Jofre, G. I., D'Agostino, E. R. R., Mavengere, H., Tate, A. D., & Matute, D. R. (2022). A need for standardized reporting of introgression: Insights from studies across eukaryotes. *Evolution Letters*, *6*(5), 344–357. https://doi.org/10.1002/evl3.294

Damgaard, P. B., Margaryan, A., Schroeder, H., Orlando, L., Willerslev, E., & Allentoft, M. E. (2015). Improving access to endogenous DNA in ancient bones and teeth. *Scientific Reports*, *5*(1), 11184. https://doi.org/10.1038/srep11184

Danecek, P., Auton, A., Abecasis, G., Albers, C. A., Banks, E., DePristo, M. A., Handsaker, R. E., Lunter, G., Marth, G. T., Sherry, S. T., McVean, G., Durbin, R., & 1000 Genomes Project Analysis Group. (2011). The variant call format and VCFtools. *Bioinformatics*, *27*(15), 2156–2158. https://doi.org/10.1093/bioinformatics/btr330

Delph, L. F., & Kelly, J. K. (2014). On the importance of balancing selection in plants. *The New Phytologist*, *201*(1), 10.1111/nph.12441. https://doi.org/10.1111/nph.12441

Di Natale, A. (2015). *REVIEW OF THE HISTORICAL AND BIOLOGICAL EVIDENCES ABOUT A POPULATION OF BLUEFIN TUNA (*THUNNUS THYNNUS L.*) IN THE EASTERN MEDITERRANEAN AND THE BLACK SEA*. ICCAT. https://www.iccat.int/Documents/CVSP/CV071_2015/n_3/CV071031098.pdf

Díaz-Arce, N., Arrizabalaga, H., Murua, H., Irigoien, X., & Rodríguez-Ezpeleta, N. (2016). RAD-seq derived genome-wide nuclear markers resolve the phylogeny of tunas. *Molecular Phylogenetics and Evolution*, *102*, 202–207. https://doi.org/10.1016/j.ympev.2016.06.002

Díaz-Arce, N., Gagnaire, P.-A., Richardson, D. E., Walter III, J. F., Arnaud-Haond, S., Fromentin, J.-M., Brophy, D., Lutcavage, M., Addis, P., Alemany, F., Allman, R., Deguara, S., Fraile, I., Goñi, N., Hanke, A. R., Karakulak, F. S., Pacicco, A., Quattro, J. M., Rooker, J. R., … Rodríguez-Ezpeleta, N. (2024). Unidirectional trans-Atlantic gene flow and a mixed spawning area shape the genetic connectivity of Atlantic bluefin tuna. *Molecular Ecology, 33(1)*, e17188. https://doi.org/10.1111/mec.17188

Donaldson, K. A., & Wilson, R. R. (1999). Amphi-Panamic Geminates of Snook (Percoidei: Centropomidae) Provide a Calibration of the Divergence Rate in the Mitochondrial DNA Control Region of Fishes. *Molecular Phylogenetics and Evolution*, *13*(1), 208–213. https://doi.org/10.1006/mpev.1999.0625

Duranton, M., Allal, F., Valière, S., Bouchez, O., Bonhomme, F., & Gagnaire, P.-A. (2020). The contribution of ancient admixture to reproductive isolation between European sea bass lineages. *Evolution Letters*, *4*(3), 226–242. https://doi.org/10.1002/evl3.169

Excoffier, L., & Lischer, H. E. L. (2010). Arlequin suite ver 3.5: A new series of programs to perform population genetics analyses under Linux and Windows. *Molecular Ecology Resources*, *10*(3), 564–567. https://doi.org/10.1111/j.1755-0998.2010.02847.x

Faillettaz, R., Beaugrand, G., Goberville, E., & Kirby, R. R. (2019). Atlantic Multidecadal Oscillations drive the basin-scale distribution of Atlantic bluefin tuna. *Science Advances*, *5*(1), eaar6993. https://doi.org/10.1126/sciadv.aar6993

Ferrari, G., Cuevas, A., Gondek-Wyrozemska, A. T., Ballantyne, R., Kersten, O., Pálsdóttir, A. H., van der Jagt, I., Hufthammer, A. K., Ystgaard, I., Wickler, S., Bigelow, G. F., Harland, J., Nicholson, R., Orton, D., Clavel, B., Boessenkool, S., Barrett, J. H., & Star, B. (2021). The preservation of ancient DNA in archaeological fish bone. Journal of Archaeological Science, 126, 105317. https://doi.org/10.1016/j.jas.2020.105317

Fijarczyk, A., & Babik, W. (2015). Detecting balancing selection in genomes: Limits and prospects. *Molecular Ecology*, *24*(14), 3529–3545. https://doi.org/10.1111/mec.13226

Fiksen, Ø., & Reglero, P. (2022). Atlantic bluefin tuna spawn early to avoid metabolic meltdown in larvae. *Ecology*, *103*(1), e03568. https://doi.org/10.1002/ecy.3568

Fromentin, J.-M., Reygondeau, G., Bonhommeau, S., & Beaugrand, G. (2014). Oceanographic changes and exploitation drive the spatio-temporal dynamics of Atlantic bluefin tuna (*Thunnus thynnus*). *Fisheries Oceanography*, *23*(2), 147–156. https://doi.org/10.1111/fog.12050

Fu, Y. X., & Li, W. H. (1993). Statistical tests of neutrality of mutations. *Genetics*, *133*(3), 693–709. https://doi.org/10.1093/genetics/133.3.693

García A, Cortés D, Quintanilla J, Rámirez T, Quintanilla L, Rodríguez JM, Alemany F. 2013 Climate-induced environmental conditions influencing interannual variability of Mediterranean bluefin (Thunnus thynnus) larval growth. *Fish. Oceanogr*. 22, 273–287. (doi:10.1111/fog.12021)

Gardner, J. P. A. (1997). Hybridization in the Sea. In J. H. S. Blaxter & A. J. Southward (Eds.), *Advances in Marine Biology* (Vol. 31, pp. 1–78). Academic Press. https://doi.org/10.1016/S0065-2881(08)60221-7

Garroway, C. J., Bowman, J., Cascaden, T. J., Holloway, G. L., Mahan, C. G., Malcolm, J. R., Steele, M. A., Turner, G., & Wilson, P. J. (2010). Climate change induced hybridization in flying squirrels. *Global Change Biology*, *16*(1), 113–121. https://doi.org/10.1111/j.1365-2486.2009.01948.x

GATK. (2016). *GATK Hands -On Tutorial: Variant Discovery with GATK*. https://qcb.ucla.edu/wp-content/uploads/sites/14/2016/03/GATK_Discovery_Tutorial-Worksheet-AUS2016.pdf

Gilbert, M. T. P., Bandelt, H.-J., Hofreiter, M., & Barnes, I. (2005). Assessing ancient DNA studies. *Trends in Ecology & Evolution*, *20*(10), 541–544. https://doi.org/10.1016/j.tree.2005.07.005

Ginolhac, A., Rasmussen, M., Gilbert, M. T. P., Willerslev, E., & Orlando, L. (2011). mapDamage: Testing for damage patterns in ancient DNA sequences. *Bioinformatics*, *27*(15), 2153–2155. https://doi.org/10.1093/bioinformatics/btr347

Gondek, A. T., Boessenkool, S., & Star, B. (2018). A stainless-steel mortar, pestle and sleeve design for the efficient fragmentation of ancient bone. *BioTechniques*, *64*(6), 266–269. https://doi.org/10.2144/btn-2018-0008

Gong, L., Liu, L.-Q., Guo, B.-Y., Ye, Y.-Y., & Lü, Z.-M. (2017). The complete mitochondrial genome characterization of Thunnus obesus (Scombriformes: Scombridae) and phylogenetic analyses of Thunnus. *Conservation Genetics Resources*, *9*(3), 379–383. https://doi.org/10.1007/s12686-017-0688-2

Hawks, J. (2017). Introgression Makes Waves in Inferred Histories of Effective Population Size. *Human Biology*, *89*(1), 67–80.

Hoffmann, A. A., & Sgrò, C. M. (2011). Climate change and evolutionary adaptation. *Nature*, *470*(7335), Article 7335. https://doi.org/10.1038/nature09670

Hohenlohe, P. A., Funk, W. C., & Rajora, O. P. (2021). Population genomics for wildlife conservation and management. *Molecular Ecology*, *30*(1), 62–82. https://doi.org/10.1111/mec.15720

Hubbs, C. L. (1955). Hybridization between Fish Species in Nature. *Systematic Biology*, *4*(1), 1–20. https://doi.org/10.2307/sysbio/4.1.1

ICCAT. (2016). Report of the 2016 ICCAT North and South Atlantic albacore stock assessment meeting. *ICCAT*. https://www.iccat.int/Documents/Meetings/Docs/2016_ALB_REPORT_ENG.pdf

ICCAT. (2020). 2020 Advice to the commission - 5.1 ALB – Atlantic Albacore. *ICCAT*. https://www.iccat.int/documents/scrs/execsum/alb_eng.pdf

ICCAT (2022a). Recommendation By ICCAT Amending The Recommendation 21-08 Establishing A Multi-Annual Management Plan For Bluefin Tuna In The Eastern Atlantic And The Mediterranean (Rec-22-08).

ICCAT (2022b). Recommendation By ICCAT Establishing A Management Procedure For Atlantic Bluefin Tuna To Be Used For Both The Western Atlantic And Eastern Atlantic And Mediterranean Management Areas (Rec 22-09).

ICCAT. (2023). *REPORT for biennial period, 2022-23 PART I (2022)—Vol. 3 Annual Reports*. ICCAT. https://www.iccat.int/Documents/BienRep/REP_TRILINGUAL_22-23_I_3.pdf

IMR. (2021, October 29). *Makrellstørje*. Havforskningsinstituttet (Institute of Marine research), Bergen, Norway. https://www.hi.no/hi/temasider/arter/makrellstorje

Jombart, T. (2008). adegenet: A R package for the multivariate analysis of genetic markers. *Bioinformatics*, *24*(11), 1403–1405. https://doi.org/10.1093/bioinformatics/btn129

Jónsson, H., Ginolhac, A., Schubert, M., Johnson, P. L. F., & Orlando, L. (2013). mapDamage2.0: Fast approximate Bayesian estimates of ancient DNA damage parameters. *Bioinformatics*, *29*(13), 1682–1684. https://doi.org/10.1093/bioinformatics/btt193

Kalyaanamoorthy, S., Minh, B. Q., Wong, T. K., von Haeseler, A., & Jermiin, L. S. (2017). ModelFinder: Fast Model Selection for Accurate Phylogenetic Estimates. *Nature Methods*, *14*(6), 587–589. https://doi.org/10.1038/nmeth.4285

Kapp, J. D., Green, R. E., & Shapiro, B. (2021). A Fast and Efficient Single-stranded Genomic Library Preparation Method Optimized for Ancient DNA. *Journal of Heredity*, *112*(3), 241–249. https://doi.org/10.1093/jhered/esab012

Kardos, M., Armstrong, E. E., Fitzpatrick, S. W., Hauser, S., Hedrick, P. W., Miller, J. M., Tallmon, D. A., & Funk, W. C. (2021). The crucial role of genome-wide genetic variation in conservation. *Proceedings of the National Academy of Sciences*, *118*(48), e2104642118. https://doi.org/10.1073/pnas.2104642118

Katoh, K., Misawa, K., Kuma, K., & Miyata, T. (2002). MAFFT: A novel method for rapid multiple sequence alignment based on fast Fourier transform. *Nucleic Acids Research*, *30*(14), 3059–3066. https://doi.org/10.1093/nar/gkf436

Kersten, O., Star, B., Krabberød, A. K., Atmore, L. M., Tørresen, O. K., Anker-Nilssen, T., Descamps, S., Strøm, H., Ulf S. Johansson, Sweet, P. R., Jakobsen, K. S., & Boessenkool, S. (2023). Hybridization of Atlantic puffins in the Arctic coincides with 20th-century climate change. Science Advances, 9(40), https://doi.org/10.1126/sciadv.adh1407

Knaus, B. J., & Grünwald, N. J. (2017). vcfr: A package to manipulate and visualize variant call format data in R. *Molecular Ecology Resources*, *17*(1), 44–53. https://doi.org/10.1111/1755-0998.12549

Kodama, Y., Shumway, M., Leinonen, R., & International Nucleotide Sequence Database Collaboration. (2012). The Sequence Read Archive: Explosive growth of sequencing data. *Nucleic Acids Research*, *40*(Database issue), D54-56. https://doi.org/10.1093/nar/gkr854

Kontopoulos, I., Penkman, K., McAllister, G. D., Lynnerup, N., Damgaard, P. B., Hansen, H. B., Allentoft, M. E., & Collins, M. J. (2019). Petrous bone diagenesis: A multi-analytical approach. Palaeogeography, Palaeoclimatology, Palaeoecology, 518, 143–154. https://doi.org/10.1016/j.palaeo.2019.01.005

Le Moan, A., Gagnaire, P.-A., & Bonhomme, F. (2016). Parallel genetic divergence among coastal–marine ecotype pairs of European anchovy explained by differential introgression after secondary contact. *Molecular Ecology*, *25*(13), 3187–3202. https://doi.org/10.1111/mec.13627

Li, H. (2011). Tabix: Fast retrieval of sequence features from generic TAB-delimited files. *Bioinformatics*, *27*(5), 718–719. https://doi.org/10.1093/bioinformatics/btq671

Li, H., & Durbin, R. (2009). Fast and accurate short read alignment with Burrows–Wheeler transform. *Bioinformatics*, *25*(14), 1754–1760. https://doi.org/10.1093/bioinformatics/btp324

Li, H., Handsaker, B., Wysoker, A., Fennell, T., Ruan, J., Homer, N., Marth, G., Abecasis, G., Durbin, R., & 1000 Genome Project Data Processing Subgroup. (2009). The Sequence Alignment/Map format and SAMtools. *Bioinformatics*, *25*(16), 2078–2079. https://doi.org/10.1093/bioinformatics/btp352

Llamas, B., Valverde, G., Fehren-Schmitz, L., Weyrich, L. S., Cooper, A., & Haak, W. (2017). From the field to the laboratory: Controlling DNA contamination in human ancient DNA research in the high-throughput sequencing era. *STAR: Science & Technology of Archaeological Research*, *3*(1), 1–14. https://doi.org/10.1080/20548923.2016.1258824

MacKenzie, B. R., Mosegaard, H., & Rosenberg, A. A. (2009). Impending collapse of bluefin tuna in the Northeast Atlantic and Mediterranean. *Conservation Letters*, *2*(1), 26–35. https://doi.org/10.1111/j.1755-263X.2008.00039.x

MacKenzie, B. R., Payne, M. R., Boje, J., Høyer, J. L., & Siegstad, H. (2014). A cascade of warming impacts brings bluefin tuna to Greenland waters. *Global Change Biology*, *20*(8), 2484–2491. https://doi.org/10.1111/gcb.12597

Martínez-García, L., Ferrari, G., Oosting, T., Ballantyne, R., van der Jagt, I., Ystgaard, I., Harland, J., Nicholson, R., Hamilton-Dyer, S., Baalsrud, H. T., Brieuc, M. S. O., Atmore, L. M., Burns, F., Schmölcke, U., Jakobsen, K. S., Jentoft, S., Orton, D., Hufthammer, A. K., Barrett, J. H., & Star, B. (2021). *Historical Demographic Processes Dominate Genetic Variation in Ancient Atlantic Cod Mitogenomes*. https://doi.org/10.17863/CAM.71522

Matschiner, M. (2016). Fitchi: Haplotype genealogy graphs based on the Fitch algorithm. *Bioinformatics*, *32*(8), 1250–1252. https://doi.org/10.1093/bioinformatics/btv717

McKenna, A., Hanna, M., Banks, E., Sivachenko, A., Cibulskis, K., Kernytsky, A., Garimella, K., Altshuler, D., Gabriel, S., Daly, M., & DePristo, M. A. (2010). The Genome Analysis Toolkit: A MapReduce framework for analyzing next-generation DNA sequencing data. *Genome Research*, *20*(9), 1297–1303. https://doi.org/10.1101/gr.107524.110

Meyer, M., & Kircher, M. (2010). Illumina Sequencing Library Preparation for Highly Multiplexed Target Capture and Sequencing. *Cold Spring Harbor Protocols*, *2010*(6), pdb.prot5448. https://doi.org/10.1101/pdb.prot5448

Montanari, S. R., Hobbs, J.-P. A., Pratchett, M. S., & van Herwerden, L. (2016). The importance of ecological and behavioural data in studies of hybridisation among marine fishes. *Reviews in Fish Biology and Fisheries*, *26*(2), 181–198. https://doi.org/10.1007/s11160-016-9420-7

Muhlfeld, C. C., Kovach, R. P., Jones, L. A., Al-Chokhachy, R., Boyer, M. C., Leary, R. F., Lowe, W. H., Luikart, G., & Allendorf, F. W. (2014). Invasive hybridization in a threatened species is accelerated by climate change. *Nature Climate Change*, *4*(7), Article 7. https://doi.org/10.1038/nclimate2252

Muhling, B. A., Lee, S.-K., Lamkin, J. T., & Liu, Y. (2011). Predicting the effects of climate change on bluefin tuna (*Thunnus thynnus*) spawning habitat in the Gulf of Mexico. *ICES Journal of Marine Science*, *68*(6), 1051–1062. https://doi.org/10.1093/icesjms/fsr008

Nguyen, L.-T., Schmidt, H. A., von Haeseler, A., & Minh, B. Q. (2015). IQ-TREE: A Fast and Effective Stochastic Algorithm for Estimating Maximum-Likelihood Phylogenies. *Molecular Biology and Evolution*, *32*(1), 268–274. https://doi.org/10.1093/molbev/msu300

Nielsen, S. V. (2020a). *Myrfunn fra Jortveit. Rapport 1 av 3. Jortveit, 172/2, Grimstad, Agder.* https://www.duo.uio.no/handle/10852/85693

Nielsen, S. V. (2020b). *Myrfunn fra Jortveit. Rapport 2 av 3. Jortveit, 172/2, Grimstad, Agder.* https://www.duo.uio.no/handle/10852/85694

Nielsen, S. V. (2020c). *Myrfunn fra Jortveit. Rapport 3 av 3. Jortveit, 172/2, Grimstad, Agder.* https://www.duo.uio.no/handle/10852/85695

Nielsen, S. V., & Persson, P. (2020). The Jortveit farm wetland: A Neolithic fishing site on the Skagerrak coast, Norway. *Journal of Wetland Archaeology*, *0*(0), 1–24. https://doi.org/10.1080/14732971.2020.1776495

NOAA. (2023, May 18). *North Atlantic Albacore Tuna | NOAA Fisheries* (New England/Mid-Atlantic,Southeast). NOAA. https://www.fisheries.noaa.gov/species/north-atlantic-albacore-tuna

Nøttestad, L., Boge, E., & Ferter, K. (2020). The comeback of Atlantic bluefin tuna (*Thunnus thynnus*) to Norwegian waters. *Fisheries Research*, *231*, 105689. https://doi.org/10.1016/j.fishres.2020.105689

Oosting, T., Martínez-García, L., Ferrari, G., Verry, A. J. F., Scarsbrook, L., Rawlence, N. J., Wellenreuther, M., Star, B., & Ritchie, P. A. (2023). Mitochondrial genomes reveal mid-Pleistocene population divergence, and post-glacial expansion, in Australasian snapper (*Chrysophrys auratus*). *Heredity*, *130*(1), Article 1. https://doi.org/10.1038/s41437-022-00579-1

Ottenburghs, J. (2021). The genic view of hybridization in the Anthropocene. *Evolutionary Applications*, *14*(10), 2342–2360. https://doi.org/10.1111/eva.13223

Paradis, E. (2010). pegas: An R package for population genetics with an integrated–modular approach. *Bioinformatics*, *26*(3), 419–420. https://doi.org/10.1093/bioinformatics/btp696

Paradis, E., Claude, J., & Strimmer, K. (2004). APE: Analyses of Phylogenetics and Evolution in R language. *Bioinformatics*, *20*(2), 289–290. https://doi.org/10.1093/bioinformatics/btg412

Pons, J.-M., Sonsthagen, S., Dove, C., & Crochet, P.-A. (2014). Extensive mitochondrial introgression in North American Great Black-backed Gulls (*Larus marinus*) from the American Herring Gull (*Larus smithsonianus*) with little nuclear DNA impact. *Heredity*, *112*(3), Article 3. https://doi.org/10.1038/hdy.2013.98

Potts, W. M., Henriques, R., Santos, C. V., Munnik, K., Ansorge, I., Dufois, F., Booth, A. J., Kirchner, C., Sauer, W. H. H., & Shaw, P. W. (2014). Ocean warming, a rapid distributional shift, and the hybridization of a coastal fish species. *Global Change Biology*, *20*(9), 2765–2777. https://doi.org/10.1111/gcb.12612

Rambaut, A. (2018, November 26). *FigTree v1.4.4*. GitHub. https://github.com/rambaut/figtree/releases

907 Rambaut, A., Drummond, A. J., Xie, D., Baele, G., & Suchard, M. A. (2018). Posterior Summarization in
908 Bayesian Phylogenetics Using Tracer 1.7. *Systematic Biology*, *67*(5), 901–904.
909 https://doi.org/10.1093/sysbio/syy032
910 Ravier, C., & Fromentin, J.-M. (2004). Are the long-term fluctuations in Atlantic bluefin tuna (Thunnus thynnus)
911 population related to environmental changes? *Fisheries Oceanography*, *13*(3), 145–160.
912 https://doi.org/10.1111/j.1365-2419.2004.00284.x
913 Reglero, P., Balbin, R., Abascal, F. J., Medina, A., Alvarez-Berastegui, D., Rasmuson, L., Mourre, B., Saber, S.,
914 Ortega, A., Blanco, E., de la Gandara, F., Alemany, F. J., Ingram, G. W., Hidalgo, M. Pelagic habitat
915 and offspring survival in the eastern stock of Atlantic bluefin tuna. – *ICES Journal of Marine Science*,
916 doi:10.1093/icesjms/fsy135.
917 Rhymer, J. M., & Simberloff, D. (1996). Extinction by Hybridization and Introgression. *Annual Review of Ecology*
918 *and Systematics*, *27*(1), 83–109. https://doi.org/10.1146/annurev.ecolsys.27.1.83
919 Rodriguez, A. K., & Krug, P. J. (2022). Ecological speciation by sympatric host shifts in a clade of herbivorous
920 sea slugs, with introgression and localized mitochondrial capture between species. *Molecular*
921 *Phylogenetics and Evolution*, *174*, 107523. https://doi.org/10.1016/j.ympev.2022.107523
922 Rodríguez-Ezpeleta, N., Díaz-Arce, N., Walter, J. F., Richardson, D. E., Rooker, J. R., Nøttestad, L., Hanke, A.
923 R., Franks, J. S., Deguara, S., Lauretta, M. V., Addis, P., Varela, J. L., Fraile, I., Goñi, N., Abid, N.,
924 Alemany, F., Oray, I. K., Quattro, J. M., Sow, F. N., … Arrizabalaga, H. (2019). Determining natal origin
925 for improved management of Atlantic bluefin tuna. *Frontiers in Ecology and the Environment*, *17*(8),
926 439–444. https://doi.org/10.1002/fee.2090
927 Rooker, J. R., Alvarado Bremer, J. R., Block, B. A., Dewar, H., de Metrio, G., Corriero, A., Kraus, R. T., Prince,
928 E. D., Rodríguez-Marín, E., & Secor, D. H. (2007). Life History and Stock Structure of Atlantic Bluefin
929 Tuna (*Thunnus thynnus*). *Reviews in Fisheries Science*, *15*(4), 265–310.
930 https://doi.org/10.1080/10641260701484135
931 Roques, Sé., SÉvigny, J.-M., & Bernatchez, L. (2001). Evidence for broadscale introgressive hybridization
932 between two redfish (genus Sebastes) in the North-West Atlantic: A rare marine example. *Molecular*
933 *Ecology*, *10*(1), 149–165. https://doi.org/10.1046/j.1365-294X.2001.01195.x
934 Rozas, J., Ferrer-Mata, A., Sánchez-DelBarrio, J. C., Guirao-Rico, S., Librado, P., Ramos-Onsins, S. E., &
935 Sánchez-Gracia, A. (2017). DnaSP 6: DNA Sequence Polymorphism Analysis of Large Data Sets.
936 *Molecular Biology and Evolution*, *34*(12), 3299–3302. https://doi.org/10.1093/molbev/msx248
937 Ryan, S. F., Deines, J. M., Scriber, J. M., Pfrender, M. E., Jones, S. E., Emrich, S. J., & Hellmann, J. J. (2018).
938 Climate-mediated hybrid zone movement revealed with genomics, museum collection, and simulation
939 modeling. *Proceedings of the National Academy of Sciences*, *115*(10), E2284–E2291.
940 https://doi.org/10.1073/pnas.1714950115
941 Saber, S., Urbina, J. O. de, Gómez-Vives, M. J., & Macías, D. (2015). Some aspects of the reproductive biology
942 of albacore *Thunnus alalunga* from the Western Mediterranean Sea. *Journal of the Marine Biological*
943 *Association of the United Kingdom*, *95*(8), 1705–1715. https://doi.org/10.1017/S002531541500020X
944 Santini, F., Carnevale, G., & Sorenson, L. (2013). First molecular scombrid timetree (Percomorpha:
945 Scombridae) shows recent radiation of tunas following invasion of pelagic habitat. *Italian Journal*
946 *of Zoology*, *80*(2), 210–221. https://doi.org/10.1080/11250003.2013.775366
947 Schroeder, H., Ávila-Arcos, M. C., Malaspinas, A.-S., Poznik, G. D., Sandoval-Velasco, M., Carpenter, M. L.,
948 Moreno-Mayar, J. V., Sikora, M., Johnson, P. L. F., Allentoft, M. E., Samaniego, J. A., Haviser, J. B.,
949 Dee, M. W., Stafford, T. W., Salas, A., Orlando, L., Willerslev, E., Bustamante, C. D., & Gilbert, M. T.
950 P. (2015). Genome-wide ancestry of 17th-century enslaved Africans from the Caribbean. *Proceedings*
951 *of the National Academy of Sciences*, *112*(12), 3669–3673. https://doi.org/10.1073/pnas.1421784112
952 Schubert, M., Ermini, L., Sarkissian, C. D., Jónsson, H., Ginolhac, A., Schaefer, R., Martin, M. D., Fernández,
953 R., Kircher, M., McCue, M., Willerslev, E., & Orlando, L. (2014). Characterization of ancient and
954 modern genomes by SNP detection and phylogenomic and metagenomic analysis using PALEOMIX.
955 *Nature Protocols*, *9*(5), Article 5. https://doi.org/10.1038/nprot.2014.063
956 Schubert, M., Lindgreen, S., & Orlando, L. (2016). AdapterRemoval v2: Rapid adapter trimming, identification,
957 and read merging. *BMC Research Notes*, *9*(1), 88. https://doi.org/10.1186/s13104-016-1900-2
958 Schwarz, G. (1978). Estimating the Dimension of a Model. *The Annals of Statistics*, *6*(2), 461–464.
959 SCRS. (2021). *Report for biennial period 2020-21 PART I (2020)—Vol. 1 English version*. ICCAT.
960 https://www.iccat.int/Documents/BienRep/REP_EN_20-21_I-1.pdf
961 SCRS. (2023). *REPORT for biennial period, 2022-23 PART I (2022)—Vol. 2*. ICCAT.
962 https://www.iccat.int/Documents/BienRep/REP_EN_22-23-I-2.pdf
963 Seixas, F. A., Boursot, P., & Melo-Ferreira, J. (2018). The genomic impact of historical hybridization with
964 massive mitochondrial DNA introgression. *Genome Biology*, *19*(1), 91. https://doi.org/10.1186/s13059-
965 018-1471-8

Semenova, A. V. (2020). Introgressive Hybridization in the Secondary Contact Area of the Atlantic Herring *Clupea harengus* and the Pacific Herring *C. pallasii* (Clupeidae): Ecological Basis, Geographical Structure, and Temporal Variability of the Hybridization Zone. *Journal of Ichthyology*, *60*(4), 626–642. https://doi.org/10.1134/S0032945220030169

Shen, W., Le, S., Li, Y., & Hu, F. (2016). SeqKit: A Cross-Platform and Ultrafast Toolkit for FASTA/Q File Manipulation. *PLOS ONE*, *11*(10), e0163962. https://doi.org/10.1371/journal.pone.0163962

Sloan, D. B., Havird, J. C., & Sharbrough, J. (2017). The on-again, off-again relationship between mitochondrial genomes and species boundaries. *Molecular Ecology*, *26*(8), 2212–2236. https://doi.org/10.1111/mec.13959

Suda, A., Nishiki, I., Iwasaki, Y., Matsuura, A., Akita, T., Suzuki, N., & Fujiwara, A. (2019). Improvement of the Pacific bluefin tuna (*Thunnus orientalis*) reference genome and development of male-specific DNA markers. *Scientific Reports*, *9*(1), Article 1. https://doi.org/10.1038/s41598-019-50978-4

Szpak, P. (2011). Fish bone chemistry and ultrastructure: Implications for taphonomy and stable isotope analysis. Journal of Archaeological Science, 38(12), 3358–3372. https://doi.org/10.1016/j.jas.2011.07.022

Tajima, F. (1989). Statistical method for testing the neutral mutation hypothesis by DNA polymorphism. *Genetics*, *123*(3), 585–595. https://doi.org/10.1093/genetics/123.3.585

Tangen, M. (2009). The Norwegian Fishery for Atlantic Bluefin tuna. *ICCAT Collect. Vol. Sci. Pap. ICCAT, 63: 79-93* (2009). https://www.iccat.int/Documents/CVSP/CV063_2009/n_1/CVOL63010079.pdf

Taylor, S. A., & Larson, E. L. (2019). Insights from genomes into the evolutionary importance and prevalence of hybridization in nature. *Nature Ecology & Evolution*, *3*(2), Article 2. https://doi.org/10.1038/s41559-018-0777-y

Toews, D. P. L., & Brelsford, A. (2012). The biogeography of mitochondrial and nuclear discordance in animals. *Molecular Ecology*, *21*(16), 3907–3930. https://doi.org/10.1111/j.1365-294X.2012.05664.x

Tseng, M.-C., Shiao, J.-C., & Hung, Y.-H. (2011). Genetic identification of *Thunnus orientalis*, *T. thynnus*, and *T. maccoyii* by a cytochrome b gene analysis. *Environmental Biology of Fishes*, *91*(1), 103–115. https://doi.org/10.1007/s10641-010-9764-0

Turbek, S. P., & Taylor, S. A. (2023). Hybridization provides climate resilience. *Nature Climate Change*, *13*(3), Article 3. https://doi.org/10.1038/s41558-022-01586-0

Vandeputte, M., Gagnaire, P.-A., & Allal, F. (2019). The European sea bass: A key marine fish model in the wild and in aquaculture. *Animal Genetics*, *50*(3), 195–206. https://doi.org/10.1111/age.12779

Vera, M., Aparicio, E., Heras, S., Abras, A., Casanova, A., Roldán, M.-I., & García-Marin, J.-L. (2023). Regional environmental and climatic concerns on preserving native gene pools of a least concern species: Brown trout lineages in Mediterranean streams. *Science of The Total Environment*, *862*, 160739. https://doi.org/10.1016/j.scitotenv.2022.160739

Viñas, J., Gordoa, A., Fernández-Cebrián, R., Pla, C., Vahdet, Ü., & Araguas, R. M. (2011). Facts and uncertainties about the genetic population structure of Atlantic bluefin tuna (*Thunnus thynnus*) in the Mediterranean. Implications for fishery management. *Reviews in Fish Biology and Fisheries*, *21*(3), 527–541. https://doi.org/10.1007/s11160-010-9174-6

Viñas, J., Pla, C., Tawil, M. Y., Hattour, A., & Farrugia, A. F. (2003). *Mitochondrial Genetic Characterization Of Bluefin Tuna (Thunnus Thynnus) From Three Mediterranean (Libya, Malta, Tunisia); And One Atlantic Locations (Gulf Of Cadiz)*. 7.

Viñas, J., & Tudela, S. (2009). A Validated Methodology for Genetic Identification of Tuna Species (Genus *Thunnus*). *PLoS ONE*, *4*(10), e7606. https://doi.org/10.1371/journal.pone.0007606

Wang, P., Dong, N., Wang, M., Sun, G., Jia, Y., Geng, X., Liu, M., Wang, W., Pan, Z., Yang, Q., Li, H., Wei, C., Wang, L., Zheng, H., He, S., Zhang, X., Wang, Q., & Du, X. (2022). Introgression from *Gossypium hirsutum* is a driver for population divergence and genetic diversity in *Gossypium barbadense*. *The Plant Journal*, *110*(3), 764–780. https://doi.org/10.1111/tpj.15702

Wickham, H., Averick, M., Bryan, J., Chang, W., McGowan, L. D., François, R., Grolemund, G., Hayes, A., Henry, L., Hester, J., Kuhn, M., Pedersen, T. L., Miller, E., Bache, S. M., Müller, K., Ooms, J., Robinson, D., Seidel, D. P., Spinu, V., … Yutani, H. (2019). Welcome to the Tidyverse. *Journal of Open Source Software*, *4*(43), 1686. https://doi.org/10.21105/joss.01686

Willi, Y., Kristensen, T. N., Sgrò, C. M., Weeks, A. R., Ørsted, M., & Hoffmann, A. A. (2022). Conservation genetics as a management tool: The five best-supported paradigms to assist the management of threatened species. *Proceedings of the National Academy of Sciences*, *119*(1), e2105076119. https://doi.org/10.1073/pnas.2105076119

Worm, B., & Tittensor, D. P. (2011). Range contraction in large pelagic predators. *Proceedings of the National Academy of Sciences*, *108*(29), 11942–11947. https://doi.org/10.1073/pnas.1102353108

Xuereb, A., D'Aloia, C. C., Andrello, M., Bernatchez, L., & Fortin, M.-J. (2021). Incorporating putatively neutral and adaptive genomic data into marine conservation planning. *Conservation Biology*, *35*(3), 909–920. https://doi.org/10.1111/cobi.13609

Supplementary

Supplementary Section 1

R-packages used in population genomic analyses

- vcfR (data loading) (Knaus & Grünwald, 2017)
- adegenet (ordination analysis) (Jombart, 2008)
- ape (phylogenetic analyses) (Paradis et al., 2004)
- pegas (population genomic statistics) (Paradis, 2010)
- ggplot in tidyverse (visualization) (Wickham et al., 2019)
- gridExtra (visualization) (Auguie and Antonov 2017)
- lemon (visualization) (Edwards 2017)

Section 2: Supplementary Tables

Table S1: Sample locations, laboratory protocols and dsDNA concentration for the ancient Atlantic bluefin samples from Norway. All samples were taken from bone tissue (vertebrae) and all samples were dated by context to be from 3000 BCE. More information about the sites can be found in the archaeological reports (Nielsen, 2020a, 2020b, 2020c).

Sample-ID	Coordinates	Extraction protocol	Qubit concentration	Library protocol
aTUNn02-Norway-3000BCE	N 58.28 E 8.50	DD	1.24	M&K DS
aTUNn03-Norway-3000BCE	N 58.28 E 8.50	DD	0.48	M&K DS
aTUNn04-Norway-3000BCE	N 58.28 E 8.50	DD	1.27	M&K DS
aTUNn05-Norway-3000BCE	N 58.28 E 8.50	DD	1.02	M&K DS
aTUNn06-Norway-3000BCE	N 58.28 E 8.50	DD	2.7	M&K DS
aTUNn07-Norway-3000BCE	N 58.28 E 8.50	bleDD	n.a.	M&K DS
aTUNn08-Norway-3000BCE	N 58.28 E 8.50	bleDD	n.a.	M&K DS
aTUNn09-Norway-3000BCE	N 58.28 E 8.50	bleDD	n.a.	M&K DS
aTUNn10-Norway-3000BCE	N 58.28 E 8.50	bleDD	n.a.	M&K DS
aTUNn11-Norway-3000BCE	N 58.28 E 8.50	bleDD	n.a.	M&K DS
aTUNn12-Norway-3000BCE	N 58.28 E 8.50	bleDD	n.a.	M&K DS
aTUNn13-Norway-3000BCE	N 58.28 E 8.50	bleDD	n.a.	M&K DS
aTUNn14-Norway-3000BCE	N 58.28 E 8.50	bleDD	n.a.	M&K DS
aTUNn15-Norway-3000BCE	N 58.28 E 8.50	bleDD	n.a.	M&K DS
aTUNn16-Norway-3000BCE	N 58.28 E 8.50	bleDD	n.a.	M&K DS
aTUNn17-Norway-3000BCE	N 58.28 E 8.50	bleDD	1.28	SC SS
aTUNn18-Norway-3000BCE	N 58.28 E 8.50	bleDD	13.3	SC SS
aTUNn19-Norway-3000BCE	N 58.28 E 8.50	bleDD	5.6	SC SS
aTUNn20-Norway-3000BCE	N 58.28 E 8.50	bleDD	1.6	SC SS
aTUNn21-Norway-3000BCE	N 58.28 E 8.50	bleDD	2.8	SC SS
aTUNn22-Norway-3000BCE	N 58.28 E 8.50	bleDD	5.56	SC SS
aTUNn23-Norway-3000BCE	N 58.28 E 8.50	bleDD	19.6	SC SS
aTUNn24-Norway-3000BCE	N 58.28 E 8.50	bleDD	3.54	SC SS
aTUNn25-Norway-3000BCE	N 58.28 E 8.50	bleDD	11	SC SS
aTUNn26-Norway-3000BCE	N 58.28 E 8.50	bleDD	6.94	SC SS
aTUNn27-Norway-3000BCE	N 58.28 E 8.50	bleDD	2.8	SC SS
aTUNn28-Norway-3000BCE	N 58.28 E 8.50	bleDD	10.9	SC SS
aTUNn29-Norway-3000BCE	N 58.28 E 8.50	bleDD	89.6	SC SS
aTUNn30-Norway-3000BCE	N 58.28 E 8.50	bleDD	1.87	SC SS
aTUNn31-Norway-3000BCE	N 58.28 E 8.50	bleDD	19.9	SC SS
aTUNn32-Norway-3000BCE	N 58.28 E 8.50	bleDD	26	SC SS
aTUNn33-Norway-3000BCE	N 58.28 E 8.50	bleDD	1.9	SC SS
aTUNn34-Norway-3000BCE	N 58.28 E 8.50	bleDD	36	SC SS
aTUNn35-Norway-3000BCE	N 58.28 E 8.50	bleDD	78.8	SC SS
aTUNn36-Norway-3000BCE	N 58.28 E 8.50	bleDD	25.2	SC SS
aTUNn37-Norway-3000BCE	N 58.28 E 8.50	bleDD	3.18	SC SS
aTUNn38-Norway-3000BCE	N 58.28 E 8.50	bleDD	3.06	SC SS
aTUNn39-Norway-3000BCE	N 58.28 E 8.50	bleDD	1.4	SC SS

DD: Double digestion. Extraction protocol adapted from Damgaard et al. 2015.
bleDD: Bleach and double digestion. Extraction protocol adapted from Boessenkool et al. 2017.
M&K DS: Double stranded libraries. Library protocol adapted from Meyer and Kircher 2010 with modifications from Schroeder et al. 2015.
SC SS: Santa Cruz Reaction single-stranded library protocol from Kapp, Green, and Shapiro 2021.

Table S2: Sample locations, date sampled and for the ancient Atlantic bluefin samples from the Mediterranean. All samples were taken from bone tissue (vertebrae). Samples were dated by context at the archaeological sites. More information about the sites can be found in Andrews et al. (2023b).

Sample-ID	Coordinates	Location	Date of origin
aTUNm01-Sicily-900-1200CE	N 38.11 E 13.37	Palermo	900-1000 CE
aTUNm02-Sicily-900-1200CE	N 38.11 E 13.37	Palermo	900-1000 CE
aTUNm03-Sicily-900-1200CE	N 38.11 E 13.37	Palermo	900-1000 CE
aTUNm04-Sicily-900-1200CE	N 38.11 E 13.37	Palermo	900-1000 CE
aTUNm05-Sicily-900-1200CE	N 38.11 E 13.37	Palermo	900-1000 CE
aTUNm06-Sicily-900-1200CE	N 38.11 E 13.37	Palermo	900-1000 CE
aTUNm07-Sicily-900-1200CE	N 37.65 E 12.59	Mazara del Vallo	1200 CE
aTUNm08-Sicily-900-1200CE	N 37.65 E 12.59	Mazara del Vallo	1200 CE
aTUNm09-Sicily-900-1200CE	N 37.65 E 12.59	Mazara del Vallo	1200 CE
aTUNm10-Sicily-900-1200CE	N 37.65 E 12.59	Mazara del Vallo	1200 CE
aTUNm11-Sicily-900-1200CE	N 38.11 E 13.36	Palermo	900-1000 CE
aTUNm12-Sicily-900-1200CE	N 38.11 E 13.36	Palermo	900-1000 CE
aTUNm13-Zliten-1925CE	N 33.25 E 14.66	Zliten	1925 CE
aTUNm14-Zliten-1925CE	N 33.25 E 14.66	Zliten	1925 CE
aTUNm15-Zliten-1925CE	N 33.25 E 14.66	Zliten	1925 CE
aTUNm16-Zliten-1925CE	N 33.25 E 14.66	Zliten	1925 CE
aTUNm17-Zliten-1925CE	N 33.25 E 14.66	Zliten	1925 CE
aTUNm18-Zliten-1925CE	N 33.25 E 14.66	Zliten	1925 CE
aTUNm19-Zliten-1925CE	N 33.25 E 14.66	Zliten	1925 CE
aTUNm20-Zliten-1925CE	N 33.25 E 14.66	Zliten	1925 CE
aTUNm21-Zliten-1925CE	N 33.25 E 14.66	Zliten	1925 CE
aTUNm22-Zliten-1925CE	N 33.25 E 14.66	Zliten	1925 CE
aTUNm23-Zliten-1925CE	N 33.25 E 14.66	Zliten	1925 CE
aTUNm24-Zliten-1925CE	N 33.25 E 14.66	Zliten	1925 CE
aTUNm25-Zliten-1925CE	N 33.25 E 14.66	Zliten	1925 CE
aTUNm26-Zliten-1925CE	N 33.25 E 14.66	Zliten	1925 CE
aTUNm27-Zliten-1925CE	N 33.25 E 14.66	Zliten	1925 CE
aTUNm28-Zliten-1925CE	N 33.25 E 14.66	Zliten	1925 CE
aTUNm29-Zliten-1925CE	N 33.25 E 14.66	Zliten	1925 CE
aTUNm30-Zliten-1925CE	N 33.25 E 14.66	Zliten	1925 CE
aTUNm31-Zliten-1925CE	N 33.25 E 14.66	Zliten	1925 CE
aTUNm32-Zliten-1925CE	N 33.25 E 14.66	Zliten	1925 CE
aTUNm33-Zliten-1925CE	N 33.25 E 14.66	Zliten	1925 CE
aTUNm34-Zliten-1925CE	N 33.25 E 14.66	Zliten	1925 CE
aTUNm35-Istanbul-1941CE	N 41.01 E 28.95	Istanbul	1941 CE
aTUNm36-Istanbul-1941CE	N 41.01 E 28.95	Istanbul	1941 CE
aTUNm37-Istanbul-800-1200CE	N 41.01 E 28.95	Istanbul	800-1200 CE
aTUNm38-Istanbul-800-1200CE	N 41.01 E 28.95	Istanbul	800-1200 CE
aTUNm39-Istanbul-800-1200CE	N 41.01 E 28.95	Istanbul	800-1200 CE
aTUNm40-Istanbul-800-1200CE	N 41.01 E 28.95	Istanbul	800-1200 CE
aTUNm41-Istanbul-800-1200CE	N 41.01 E 28.95	Istanbul	800-1200 CE
aTUNm42-Istanbul-800-1200CE	N 41.01 E 28.95	Istanbul	800-1200 CE
aTUNm43-Istanbul-800-1200CE	N 41.01 E 28.95	Istanbul	800-1200 CE
aTUNm44-Istanbul-800-1200CE	N 41.01 E 28.95	Istanbul	800-1200 CE
aTUNm45-Istanbul-800-1200CE	N 41.01 E 28.95	Istanbul	800-1200 CE
aTUNm46-Istanbul-800-1200CE	N 41.01 E 28.95	Istanbul	800-1200 CE
aTUNm47-Istanbul-800-1200CE	N 41.01 E 28.95	Istanbul	800-1200 CE

aTUNm48-Istanbul-800-1200CE	N 41.01 E 28.95	Istanbul	800-1200 CE
aTUNm49-Istanbul-800-1200CE	N 41.01 E 28.95	Istanbul	800-1200 CE
aTUNm50-Istanbul-800-1200CE	N 41.01 E 28.95	Istanbul	800-1200 CE
aTUNm51-Istanbul-800-1200CE	N 41.01 E 28.95	Istanbul	800-1200 CE
aTUNm52-Istanbul-800-1200CE	N 41.01 E 28.95	Istanbul	800-1200 CE
aTUNm53-Istanbul-800-1200CE	N 41.01 E 28.95	Istanbul	800-1200 CE
aTUNm54-Istanbul-800-1200CE	N 41.01 E 28.95	Istanbul	800-1200 CE
aTUNm55-Istanbul-800-1200CE	N 41.01 E 28.95	Istanbul	800-1200 CE
aTUNm56-Istanbul-800-1200CE	N 41.01 E 28.95	Istanbul	800-1200 CE
aTUNm57-Istanbul-800-1200CE	N 41.01 E 28.95	Istanbul	800-1200 CE
aTUNm58-Gibraltar-1755CE	N 36.28 W 6.09	Conil	1755 CE
aTUNm59-Gibraltar-1755CE	N 36.28 W 6.09	Conil	1755 CE
aTUNm60-Gibraltar-1755CE	N 36.28 W 6.09	Conil	1755 CE
aTUNm61-Gibraltar-1755CE	N 36.28 W 6.09	Conil	1755 CE
aTUNm62-Gibraltar-1755CE	N 36.28 W 6.09	Conil	1755 CE
aTUNm63-Gibraltar-1755CE	N 36.28 W 6.09	Conil	1755 CE
aTUNm64-Gibraltar-1755CE	N 36.28 W 6.09	Conil	1755 CE
aTUNm65-Marseille-1800CE	N 43.30 E 5.37	Marseille	1800 CE
aTUNm66-Marseille-1800CE	N 43.30 E 5.37	Marseille	1800 CE
aTUNm67-Marseille-1800CE	N 43.30 E 5.37	Marseille	1800 CE
aTUNm68-Marseille-1800CE	N 43.30 E 5.37	Marseille	1800 CE
aTUNm69-Marseille-1800CE	N 43.30 E 5.37	Marseille	1800 CE
aTUNm70-Marseille-1800CE	N 43.30 E 5.37	Marseille	1800 CE
aTUNm71-Marseille-1800CE	N 43.30 E 5.37	Marseille	1800 CE
aTUNm72-Marseille-1800CE	N 43.30 E 5.37	Marseille	1800 CE
aTUNm73-Gibraltar-100CE	N 36.53 W 6.30	Cadiz	100 CE
aTUNm74-Gibraltar-100CE	N 36.53 W 6.30	Cadiz	100 CE
aTUNm75-Gibraltar-100CE	N 36.53 W 6.30	Cadiz	100 CE
aTUNm76-Gibraltar-100CE	N 36.53 W 6.30	Cadiz	100 CE
aTUNm77-Gibraltar-100CE	N 36.53 W 6.30	Cadiz	100 CE
aTUNm78-Sardinia-1500-1700CE	N 40.86 E 8.62	Sassari	1500-1700 CE
aTUNm79-Sardinia-1500-1700CE	N 40.86 E 8.62	Sassari	1500-1700 CE
aTUNm80-Sardinia-1500-1700CE	N 40.86 E 8.62	Sassari	1500-1700 CE
aTUNm81-Sardinia-1500-1700CE	N 40.86 E 8.62	Sassari	1500-1700 CE
aTUNm82-Sardinia-1500-1700CE	N 40.86 E 8.62	Sassari	1500-1700 CE
aTUNm83-Sardinia-1500-1700CE	N 40.86 E 8.62	Sassari	1500-1700 CE
aTUNm84-Sardinia-1500-1700CE	N 40.86 E 8.62	Sassari	1500-1700 CE
aTUNm85-Sardinia-1500-1700CE	N 40.86 E 8.62	Sassari	1500-1700 CE
aTUNm86-Sardinia-1500-1700CE	N 40.86 E 8.62	Sassari	1500-1700 CE
aTUNm87-Sardinia-1500-1700CE	N 40.86 E 8.62	Sassari	1500-1700 CE
aTUNm88-Sardinia-1500-1700CE	N 40.86 E 8.62	Sassari	1500-1700 CE
aTUNm89-Sardinia-1500-1700CE	N 40.86 E 8.62	Sassari	1500-1700 CE
aTUNm90-Sardinia-1500-1700CE	N 40.86 E 8.62	Sassari	1500-1700 CE
aTUNm91-Sardinia-1500-1700CE	N 40.86 E 8.62	Sassari	1500-1700 CE
aTUNm92-Sardinia-1500-1700CE	N 40.86 E 8.62	Sassari	1500-1700 CE

Table S3: Sample locations, lifestage, tissue, date sampled and dsDNA concentration for the modern Atlantic bluefin samples from Norway.

Sample-ID	Coordinates	Lifestage and Estimated TW (kg)	Tissue	Year sampled	Qubit concentration (ng/µl)
mTUNn01-NOR	N 63.65 E 7.95	Adult, 151.2	Powdered muscle	2018	5.5
mTUNn02-NOR	N 63.65 E 7.95	Adult, 218.6	Powdered muscle	2018	20.6
mTUNn03-NOR	N 63.65 E 7.95	Adult, 219.2	Powdered muscle	2018	20.0
mTUNn04-NOR	N 63.65 E 7.95	Adult, 225.5	Powdered muscle	2018	4.5
mTUNn05-NOR	N 63.65 E 7.95	Adult, 217.4	Powdered muscle	2018	9.2
mTUNn06-NOR	N 63.65 E 7.95	Adult, 221.1	Powdered muscle	2018	5.2
mTUNn07-NOR	N 63.65 E 7.95	Adult, 228.7	Powdered muscle	2018	10.2
mTUNn08-NOR	N 63.65 E 7.95	Adult, 227.4	Powdered muscle	2018	5.1
mTUNn09-NOR	N 63.65 E 7.95	Adult, 240.7	Powdered muscle	2018	11.7
mTUNn10-NOR	N 63.65 E 7.95	Adult, 264.0	Powdered muscle	2018	6.0
mTUNn11-NOR	N 62.90 E 6.00	Adult, 215.5	Fin skin	2020	53.4
mTUNn12-NOR	N 62.90 E 6.00	Adult, 202.9	Fin skin	2020	43.8
mTUNn13-NOR	N 62.90 E 6.00	Adult, 182.7	Fin skin	2020	31.4
mTUNn14-NOR	N 62.90 E 6.00	Adult, 313.7	Fin skin	2020	83.7
mTUNn15-NOR	N 62.90 E 6.00	Adult, 310.0	Fin skin	2020	27.3
mTUNn16-NOR	N 62.90 E 6.00	Adult, 181.4	Fin skin	2020	41.8
mTUNn17-NOR	N 62.90 E 6.00	Adult, 225.5	Fin skin	2020	13.4
mTUNn18-NOR	N 62.90 E 6.00	Adult, 170.1	Fin skin	2020	44.0
mTUNn19-NOR	N 62.90 E 6.00	Adult, 194.0	Fin skin	2020	91.9
mTUNn20-NOR	N 62.90 E 6.00	Adult, 220.5	Fin skin	2020	28.5
mTUNn21-NOR	N 62.90 E 6.00	Adult, 206.6	Fin skin	2020	81.3
mTUNn22-NOR	N 62.90 E 6.00	Adult, 250.7	Fin skin	2020	58.8
mTUNn23-NOR	N 62.90 E 6.00	Adult, 190.3	Fin skin	2020	19.1
mTUNn24-NOR	N 62.90 E 6.00	Adult, 270.9	Fin skin	2020	23.6
mTUNn25-NOR	N 62.90 E 6.00	Adult, 187.7	Fin skin	2020	73.4
mTUNn26-NOR	N 62.90 E 6.00	Adult, 186.5	Fin skin	2020	70.5
mTUNn27-NOR	N 62.90 E 6.00	Adult, 264.6	Fin skin	2020	38.7
mTUNn28-NOR	N 62.90 E 6.00	Adult, 241.9	Fin skin	2020	41.2
mTUNn29-NOR	N 62.90 E 6.00	Adult, 296.1	Fin skin	2020	48.3
mTUNn30-NOR	N 62.90 E 6.00	Adult, 260.8	Fin skin	2020	32.0
mTUNn31-NOR	N 62.90 E 6.00	Adult, 214.2	Fin skin	2020	21.8
mTUNn32-NOR	N 62.90 E 6.00	Adult, 170.1	Fin skin	2020	43.2
mTUNn33-NOR	N 62.90 E 6.00	Adult, 205.4	Fin skin	2020	36.1
mTUNn34-NOR	N 62.90 E 6.00	Adult, 181.4	Fin skin	2020	36.3
mTUNn35-NOR	N 62.90 E 6.00	Adult, 182.7	Fin skin	2020	43.8
mTUNn36-NOR	N 62.90 E 6.00	Adult, 202.9	Fin skin	2020	32.6
mTUNn37-NOR	N 62.90 E 6.00	Adult, 189.0	Fin skin	2020	66.5
mTUNn38-NOR	N 62.90 E 6.00	Adult, 204.1	Fin skin	2020	20.4

Table S4: Sample locations, lifestage, tissue and date sampled for the modern Atlantic bluefin samples from the Mediterranean and the Gulf of Mexico.

Sample-ID	Coordinates	Location	Lifestage	Year sampled
mTUNm01-EMED	N 35.51 E 33.42	Cyprus	YoY	2013
mTUNm02-EMED	N 35.51 E 33.42	Cyprus	YoY	2013
mTUNm03-EMED	N 35.51 E 33.42	Cyprus	YoY	2013
mTUNm04-EMED	N 35.51 E 33.42	Cyprus	YoY	2013
mTUNm05-EMED	N 35.51 E 33.42	Cyprus	YoY	2013
mTUNm06-EMED	N 35.51 E 33.42	Cyprus	YoY	2013
mTUNm07-EMED	N 35.51 E 33.42	Cyprus	YoY	2013
mTUNm08-EMED	N 35.51 E 33.42	Cyprus	YoY	2013
mTUNm09-EMED	N 35.51 E 33.42	Cyprus	YoY	2013
mTUNm10-EMED	N 35.51 E 33.42	Cyprus	YoY	2013
mTUNm11-WMED	N 39.27 E 2.07	Palma	YoY	2013
mTUNm12-WMED	N 39.27 E 2.07	Palma	YoY	2013
mTUNm13-WMED	N 39.27 E 2.07	Palma	YoY	2013
mTUNm14-WMED	N 39.27 E 2.07	Palma	YoY	2013
mTUNm15-WMED	N 39.27 E 2.07	Palma	YoY	2013
mTUNm16-WMED	N 39.27 E 2.07	Palma	YoY	2013
mTUNm17-WMED	N 39.27 E 2.07	Palma	YoY	2013
mTUNm18-WMED	N 39.27 E 2.07	Palma	YoY	2013
mTUNm19-WMED	N 39.27 E 2.07	Palma	YoY	2013
mTUNm20-WMED	N 39.27 E 2.07	Palma	YoY	2013
mTUNm31-CMED	N 36.93 E 13.18	Sicily	YoY	2013
mTUNm32-CMED	N 36.93 E 13.18	Sicily	YoY	2013
mTUNm33-CMED	N 36.93 E 13.18	Sicily	YoY	2013
mTUNm34-CMED	N 36.93 E 13.18	Sicily	YoY	2013
mTUNm35-CMED	N 36.93 E 13.18	Sicily	YoY	2013
mTUNm36-CMED	N 36.93 E 13.18	Sicily	YoY	2013
mTUNm37-CMED	N 36.93 E 13.18	Sicily	YoY	2013
mTUNm38-CMED	N 36.93 E 13.18	Sicily	YoY	2013
mTUNm39-CMED	N 36.93 E 13.18	Sicily	YoY	2013
mTUNm40-CMED	N 36.93 E 13.18	Sicily	YoY	2013
mTUNm41-GOM	N 26.12 W 87.78	Gulf of Mexico	larvae	2017
mTUNm42-GOM	N 25.84 W 88.13	Gulf of Mexico	larvae	2017
mTUNm43-GOM	N 28.33 W 87.25	Gulf of Mexico	larvae	2018
mTUNm44-GOM	N 28.33 W 87.25	Gulf of Mexico	larvae	2018
mTUNm45-GOM	N 28.33 W 87.25	Gulf of Mexico	larvae	2018
mTUNm46-GOM	N 26.53 W 93.58	Gulf of Mexico	larvae	2014
mTUNm47-GOM	N 26.53 W 93.58	Gulf of Mexico	larvae	2014
mTUNm48-GOM	N 27.04 W 93.00	Gulf of Mexico	larvae	2014
mTUNm49-GOM	N 28.00 W 87.76	Gulf of Mexico	larvae	2014
mTUNm50-GOM	N 28.00 W 87.76	Gulf of Mexico	larvae	2014

Table S5: Sample locations, lifestage, tissue and date sampled for the modern albacore samples from the Bay of Biscay.

Sample-ID	Coordinates	Location	Lifestage	Year sampled
ALB-TUN-01	N 44.46 W 3.12	Bay of Biscay	Juvenile (5-15 kg)	2010
ALB-TUN-02	N 44.46 W 3.12	Bay of Biscay	Juvenile (5-15 kg)	2010
ALB-TUN-03	N 44.46 W 3.12	Bay of Biscay	Juvenile (5-15 kg)	2010
ALB-TUN-04	N 44.46 W 3.12	Bay of Biscay	Juvenile (5-15 kg)	2010
ALB-TUN-05	N 44.46 W 3.12	Bay of Biscay	Juvenile (5-15 kg)	2010
ALB-TUN-06	N 44.46 W 3.12	Bay of Biscay	Juvenile (5-15 kg)	2010

Table S6: Pacific bluefin whole genome raw sequences downloaded from the DDBJ database (Kodama et al., 2012).

Original sample-ID	Sample-ID	DDBJ identifier	Filename
PAC-DRR177383	PBFT-TUN-01	DRA008331	DRR177383_1.fastq.bz2
			DRR177383_2.fastq.bz2
PAC-DRR177395	PBFT-TUN-02	DRA008331	DRR177395_1.fastq.bz2
			DRR177395_2.fastq.bz2
PAC-DRR177400	PBFT-TUN-03	DRA008331	DRR177400_1.fastq.bz2
			DRR177400_2.fastq.bz2
PAC-DRR177401	PBFT-TUN-04	DRA008331	DRR177401_1.fastq.bz2
			DRR177401_2.fastq.bz2
PAC-DRR177402	PBFT-TUN-05	DRA008331	DRR177402_1.fastq.bz2
			DRR177402_2.fastq.bz2
PAC-DRR177403	PBFT-TUN-06	DRA008331	DRR177403_1.fastq.bz2
			DRR177403_2.fastq.bz2
PAC-DRR177404	PBFT-TUN-07	DRA008331	DRR177404_1.fastq.bz2
			DRR177404_2.fastq.bz2
PAC-DRR177405	PBFT-TUN-08	DRA008331	DRR177405_1.fastq.bz2
			DRR177405_2.fastq.bz2
PAC-DRR177406	PBFT-TUN-09	DRA008331	DRR177406_1.fastq.bz2
			DRR177406_2.fastq.bz2

URL: https://ddbj.nig.ac.jp/public/ddbj_database/dra/fastq/DRA008/DRA008331/DRX167946/

Table S7: Summary statistics from Paleomix for the ancient Atlantic bluefin specimens from Norway. The endogenous content is calculated from the alignment to the Atlantic bluefin nuclear reference genome. Samples that were removed from further analyses are marked with a star (*).

Sample-ID	Reads (millions)	Endogenous DNA (fraction)	Mitochondrial coverage	Mean fragment length (bp)
aTUNn02-Norway-3000BCE	32	0.06	7	74
aTUNn03-Norway-3000BCE	42	0.15	15	64
aTUNn04-Norway-3000BCE	21	0.16	8	62
aTUNn05-Norway-3000BCE	120	0.51	164	64
aTUNn06-Norway-3000BCE	528	0.60	1546	78
aTUNn07-Norway-3000BCE	5	0.26	5	77
aTUNn08-Norway-3000BCE	16	0.14	6	66
aTUNn09-Norway-3000BCE	17	0.50	17	63
aTUNn10-Norway-3000BCE *	3	0.22	2	80
aTUNn11-Norway-3000BCE	13	0.48	14	66
aTUNn12-Norway-3000BCE *	20	0.46	18	64
aTUNn13-Norway-3000BCE	26	0.54	29	67
aTUNn14-Norway-3000BCE *	8	0.33	7	66
aTUNn15-Norway-3000BCE	10	0.17	3	70
aTUNn16-Norway-3000BCE	2	0.50	2	66
aTUNn17-Norway-3000BCE	6	0.37	11	100
aTUNn18-Norway-3000BCE *	6	0.03	1	79
aTUNn19-Norway-3000BCE	88	0.20	115	109
aTUNn20-Norway-3000BCE	19	0.32	38	101
aTUNn21-Norway-3000BCE	9	0.38	23	86
aTUNn22-Norway-3000BCE	14	0.37	34	101
aTUNn23-Norway-3000BCE	12	0.03	3	109
aTUNn24-Norway-3000BCE	153	0.64	318	91
aTUNn25-Norway-3000BCE *	14	0.23	23	81
aTUNn26-Norway-3000BCE *	11	0.17	10	95
aTUNn27-Norway-3000BCE *	16	0.34	38	85
aTUNn28-Norway-3000BCE *	15	0.04	5	97
aTUNn29-Norway-3000BCE *	13	0.09	11	106
aTUNn30-Norway-3000BCE	11	0.18	4	113
aTUNn31-Norway-3000BCE	15	0.12	13	120
aTUNn32-Norway-3000BCE *	15	0.14	12	119
aTUNn33-Norway-3000BCE *	12	0.13	12	111
aTUNn34-Norway-3000BCE *	29	0.00	0	122
aTUNn35-Norway-3000BCE	14	0.19	15	116
aTUNn36-Norway-3000BCE *	14	0.03	4	107
aTUNn37-Norway-3000BCE	344	0.64	740	77
aTUNn38-Norway-3000BCE *	25	0.47	32	90
aTUNn39-Norway-3000BCE	9	0.15	3	121

Table S8: Summary statistics from Paleomix for the ancient Atlantic bluefin specimens from the Mediterranean. The endogenous content is calculated from the alignment to the Atlantic bluefin nuclear reference genome. Samples that were removed from further analyses are marked with a star (*).

Sample-ID	Reads (millions)	Endogenous DNA (fraction)	Mitochondrial coverage	Mean fragment length (bp)
aTUNm01-Sicily-900-1200CE	16	0.07	2	83
aTUNm02-Sicily-900-1200CE	5	0.17	5	79
aTUNm03-Sicily-900-1200CE *	8	0.19	5	68
aTUNm04-Sicily-900-1200CE *	5	0.17	3	86
aTUNm05-Sicily-900-1200CE	18	0.12	10	91
aTUNm06-Sicily-900-1200CE	6	0.21	6	92
aTUNm07-Sicily-900-1200CE	6	0.52	16	86
aTUNm08-Sicily-900-1200CE	5	0.22	4	103
aTUNm09-Sicily-900-1200CE	8	0.07	2	93
aTUNm10-Sicily-900-1200CE	16	0.58	73	73
aTUNm11-Sicily-900-1200CE	7	0.59	25	79
aTUNm12-Sicily-900-1200CE	7	0.12	4	92
aTUNm13-Zliten-1925CE	7	0.38	12	70
aTUNm14-Zliten-1925CE	8	0.36	15	77
aTUNm15-Zliten-1925CE	7	0.06	3	80
aTUNm16-Zliten-1925CE	6	0.11	4	68
aTUNm17-Zliten-1925CE	6	0.33	5	69
aTUNm18-Zliten-1925CE	8	0.40	12	72
aTUNm19-Zliten-1925CE	7	0.25	6	75
aTUNm20-Zliten-1925CE	4	0.46	7	68
aTUNm21-Zliten-1925CE *	6	0.06	3	70
aTUNm22-Zliten-1925CE	8	0.37	13	67
aTUNm23-Zliten-1925CE	7	0.15	5	63
aTUNm24-Zliten-1925CE	7	0.17	4	66
aTUNm25-Zliten-1925CE	6	0.45	9	69
aTUNm26-Zliten-1925CE *	9	0.08	4	72
aTUNm27-Zliten-1925CE	8	0.07	5	83
aTUNm28-Zliten-1925CE	9	0.25	9	77
aTUNm29-Zliten-1925CE	9	0.18	6	77
aTUNm30-Zliten-1925CE	10	0.04	3	86
aTUNm31-Zliten-1925CE	7	0.49	10	80
aTUNm32-Zliten-1925CE	9	0.28	17	83
aTUNm33-Zliten-1925CE	7	0.26	6	74
aTUNm34-Zliten-1925CE	6	0.10	4	80
aTUNm35-Istanbul-1941CE	6	0.11	1	111
aTUNm36-Istanbul-1941CE	10	0.27	10	72
aTUNm37-Istanbul-800-1200CE	5	0.51	22	77
aTUNm38-Istanbul-800-1200CE	5	0.47	9	70
aTUNm39-Istanbul-800-1200CE	5	0.24	7	82
aTUNm40-Istanbul-800-1200CE *	4	0.45	19	91
aTUNm41-Istanbul-800-1200CE	5	0.57	25	76
aTUNm42-Istanbul-800-1200CE	4	0.36	7	90
aTUNm43-Istanbul-800-1200CE	4	0.32	4	74
aTUNm44-Istanbul-800-1200CE	5	0.16	3	76
aTUNm45-Istanbul-800-1200CE	4	0.59	16	75
aTUNm46-Istanbul-800-1200CE	4	0.53	18	83
aTUNm47-Istanbul-800-1200CE	4	0.61	12	77

aTUNm48-Istanbul-800-1200CE *	4	0.09	2	78
aTUNm49-Istanbul-800-1200CE	4	0.22	5	79
aTUNm50-Istanbul-800-1200CE	6	0.50	12	82
aTUNm51-Istanbul-800-1200CE	10	0.46	31	75
aTUNm52-Istanbul-800-1200CE	14	0.39	64	78
aTUNm53-Istanbul-800-1200CE	6	0.38	8	76
aTUNm54-Istanbul-800-1200CE	9	0.33	15	87
aTUNm55-Istanbul-800-1200CE	6	0.42	10	77
aTUNm56-Istanbul-800-1200CE	10	0.47	17	77
aTUNm57-Istanbul-800-1200CE	4	0.55	25	96
aTUNm58-Gibraltar-1755CE	10	0.06	2	82
aTUNm59-Gibraltar-1755CE	8	0.10	3	79
aTUNm60-Gibraltar-1755CE	6	0.10	3	87
aTUNm61-Gibraltar-1755CE	8	0.08	3	82
aTUNm62-Gibraltar-1755CE	6	0.16	2	85
aTUNm63-Gibraltar-1755CE	5	0.10	3	89
aTUNm64-Gibraltar-1755CE	14	0.06	3	83
aTUNm65-Marseille-1800CE	6	0.34	10	72
aTUNm66-Marseille-1800CE	7	0.35	69	95
aTUNm67-Marseille-1800CE	9	0.22	7	99
aTUNm68-Marseille-1800CE	10	0.24	6	82
aTUNm69-Marseille-1800CE	3	0.28	8	82
aTUNm70-Marseille-1800CE	6	0.25	12	82
aTUNm71-Marseille-1800CE	9	0.18	27	92
aTUNm72-Marseille-1800CE	38	0.12	14	72
aTUNm73-Gibraltar-100CE	22	0.05	11	92
aTUNm74-Gibraltar-100CE *	13	0.07	2	83
aTUNm75-Gibraltar-100CE	21	0.13	10	85
aTUNm76-Gibraltar-100CE	13	0.09	5	99
aTUNm77-Gibraltar-100CE	15	0.08	6	82
aTUNm78-Sardinia-1500-1700CE	5	0.39	8	103
aTUNm79-Sardinia-1500-1700CE	11	0.57	29	75
aTUNm80-Sardinia-1500-1700CE	6	0.06	4	105
aTUNm81-Sardinia-1500-1700CE	6	0.39	10	86
aTUNm82-Sardinia-1500-1700CE	5	0.40	15	93
aTUNm83-Sardinia-1500-1700CE	11	0.05	2	89
aTUNm84-Sardinia-1500-1700CE	5	0.39	14	90
aTUNm85-Sardinia-1500-1700CE	13	0.56	34	81
aTUNm86-Sardinia-1500-1700CE	7	0.14	5	99
aTUNm87-Sardinia-1500-1700CE	14	0.58	58	93
aTUNm88-Sardinia-1500-1700CE	9	0.49	13	84
aTUNm89-Sardinia-1500-1700CE	6	0.57	15	80
aTUNm90-Sardinia-1500-1700CE	10	0.59	31	87
aTUNm91-Sardinia-1500-1700CE	3	0.50	11	90
aTUNm92-Sardinia-1500-1700CE	3	0.36	7	96

1076

1077

1078

Table S9: Summary statistics from Paleomix for the modern Atlantic bluefin specimens from Norway. The endogenous content is calculated from the alignment to the Atlantic bluefin nuclear reference genome.

Sample-ID	Reads (millions)	Endogenous DNA (fraction)	Mitochondrial coverage	Mean fragment length (bp)
mTUNn01-NOR	75	0.69	2784	178
mTUNn02-NOR	59	0.73	1019	170
mTUNn03-NOR	56	0.72	1508	172
mTUNn04-NOR	79	0.75	1150	178
mTUNn05-NOR	69	0.76	823	172
mTUNn06-NOR	79	0.75	1633	169
mTUNn07-NOR	73	0.77	1163	170
mTUNn08-NOR	76	0.75	1811	175
mTUNn09-NOR	90	0.76	1960	171
mTUNn10-NOR	93	0.75	2345	171
mTUNn11-NOR	21	0.76	273	168
mTUNn12-NOR	19	0.75	307	168
mTUNn13-NOR	23	0.78	296	168
mTUNn14-NOR	19	0.76	247	170
mTUNn15-NOR	18	0.76	283	166
mTUNn16-NOR	22	0.76	370	170
mTUNn17-NOR	22	0.75	260	168
mTUNn18-NOR	33	0.75	512	169
mTUNn19-NOR	22	0.77	228	167
mTUNn20-NOR	19	0.75	251	168
mTUNn21-NOR	19	0.76	520	168
mTUNn22-NOR	17	0.77	286	166
mTUNn23-NOR	17	0.77	263	167
mTUNn24-NOR	23	0.77	301	168
mTUNn25-NOR	23	0.75	381	169
mTUNn26-NOR	21	0.76	389	169
mTUNn27-NOR	25	0.76	343	168
mTUNn28-NOR	25	0.76	349	166
mTUNn29-NOR	22	0.75	448	168
mTUNn30-NOR	23	0.77	419	169
mTUNn31-NOR	27	0.77	687	166
mTUNn32-NOR	22	0.78	543	168
mTUNn33-NOR	22	0.75	458	169
mTUNn34-NOR	18	0.76	417	166
mTUNn35-NOR	24	0.76	472	167
mTUNn36-NOR	23	0.76	356	168
mTUNn37-NOR	24	0.77	419	166
mTUNn38-NOR	24	0.75	425	169

Table S10: Summary statistics from Paleomix for the modern Atlantic bluefin specimens from the Mediterranean and the Gulf of Mexico. The endogenous content is calculated from the alignment to the Atlantic bluefin nuclear reference genome.

Sample-ID	Reads (millions)	Endogenous DNA (fraction)	Mitochondrial coverage	Mean fragment length (bp)
mTUNm01-EMED	24	0.68	716	112
mTUNm02-EMED	25	0.68	704	124
mTUNm03-EMED	22	0.69	336	118
mTUNm04-EMED	13	0.80	445	156
mTUNm05-EMED	48	0.48	2089	120
mTUNm06-EMED	37	0.49	1600	115
mTUNm07-EMED	31	0.67	708	105
mTUNm08-EMED	21	0.72	230	102
mTUNm09-EMED	19	0.71	363	100
mTUNm10-EMED	23	0.73	538	103
mTUNm11-WMED	24	0.68	1021	83
mTUNm12-WMED	27	0.70	660	112
mTUNm13-WMED	14	0.59	574	104
mTUNm14-WMED	20	0.70	396	81
mTUNm15-WMED	26	0.66	840	119
mTUNm16-WMED	46	0.61	1462	80
mTUNm17-WMED	63	0.58	1212	67
mTUNm18-WMED	60	0.57	1183	62
mTUNm19-WMED	41	0.69	410	95
mTUNm20-WMED	74	0.65	460	70
mTUNm31-CMED	36	0.35	1180	122
mTUNm32-CMED	32	0.30	666	126
mTUNm33-CMED	54	0.60	1385	69
mTUNm34-CMED	56	0.34	976	128
mTUNm35-CMED	38	0.61	448	71
mTUNm36-CMED	32	0.71	745	106
mTUNm37-CMED	45	0.55	530	104
mTUNm38-CMED	36	0.35	176	128
mTUNm39-CMED	62	0.58	705	81
mTUNm40-CMED	51	0.58	533	60
mTUNm41-GOM	80	0.66	696	69
mTUNm42-GOM	51	0.38	972	111
mTUNm43-GOM	30	0.49	565	106
mTUNm44-GOM	52	0.56	881	100
mTUNm45-GOM	44	0.47	966	128
mTUNm46-GOM	26	0.69	319	78
mTUNm47-GOM	46	0.69	49	75
mTUNm48-GOM	26	0.65	34	67
mTUNm49-GOM	67	0.55	910	102
mTUNm50-GOM	53	0.60	430	66

Table S11: Summary statistics from Paleomix for the modern albacore specimens from the Bay of Biscay. The endogenous content is calculated from the alignment to the Atlantic bluefin nuclear reference genome.

Sample-ID	Reads (millions)	Endogenous DNA (fraction)	Mitochondrial coverage	Mean fragment length (bp)
ALB-TUN-01	37	0.59	277	99
ALB-TUN-02	19	0.66	219	117
ALB-TUN-03	28	0.65	103	124
ALB-TUN-04	27	0.66	377	74
ALB-TUN-05	12	0.70	243	95
ALB-TUN-06	25	0.68	109	99

Table S12: Summary statistics from Paleomix for the modern Pacific bluefin specimens from the Nansei Islands. Whole genome raw sequence data downloaded from the DDBJ database (Kodama et al., 2012). The endogenous content is calculated from the alignment to the Atlantic bluefin nuclear reference genome.

Sample-ID	Reads (millions)	Endogenous DNA (fraction)	Mitochondrial coverage	Mean fragment length (bp)
PBFT-TUN-01	121	0.72	2657	152
PBFT-TUN-02	127	0.74	5107	151
PBFT-TUN-03	109	0.76	2346	151
PBFT-TUN-04	112	0.73	1361	151
PBFT-TUN-05	107	0.76	4005	151
PBFT-TUN-06	112	0.75	3345	151
PBFT-TUN-07	99	0.76	3061	151
PBFT-TUN-08	126	0.75	3465	151
PBFT-TUN-09	114	0.74	4555	151

Table S13: Introgressed individuals. Samples that were removed from further analyses due to being identical with other samples and/or having high missingness are marked with a star (*).

Sample-ID	Mitochondrial haplotype
aTUNn21-Norway-3000BCE	Pacific bluefin
aTUNn22-Norway-3000BCE	Pacific bluefin
aTUNn25-Norway-3000BCE *	Pacific bluefin
aTUNn26-Norway-3000BCE *	Pacific bluefin
aTUNn27-Norway-3000BCE *	Pacific bluefin
aTUNn28-Norway-3000BCE *	Pacific bluefin
aTUNn29-Norway-3000BCE *	Pacific bluefin
aTUNn33-Norway-3000BCE *	Pacific bluefin
aTUNn34-Norway-3000BCE *	Pacific bluefin
aTUNn36-Norway-3000BCE *	Pacific bluefin
aTUNm02-Sicily-900-1200CE	Albacore
aTUNm04-Sicily-900-1200CE *	Albacore
aTUNm06-Sicily-900-1200CE	Albacore
aTUNm39-Istanbul-800-1200CE	Pacific bluefin
aTUNm46-Istanbul-800-1200CE	Albacore
aTUNm81-Sardinia-1500-1700CE	Pacific bluefin
mTUNn05-NOR	Albacore
mTUNn17-NOR	Pacific bluefin
mTUNn35-NOR	Pacific bluefin
mTUNm15-WMED	Albacore

Table S14: Jointly called and filtered datasets, used in population genomic analyses (N = number of samples in each dataset).

		Location	Subset Code	N
Containing samples with signs of introgression	Modern	Norwegian sea	**NORAll**	38
		Western Mediterranean	**WMEDAll**	10
		All modern Atlantic bluefin locations	**modernABFT**	78
	Ancient	Jortveit, Norway	**Norway_3000BCE_All**	25
		Sardinia, Italy	**Sardinia_1500_1700CE_All**	15
		Istanbul, Turkey	**Istanbul_800_1200CE_All**	19
		Sicily, Italy	**Sicily_900_1200CE_All**	10
		All ancient excavation locations	**AncientAll**	109
	Both modern and ancient	All modern and ancient Atlantic bluefin locations	**AllABFT**	187
No introgressed samples present	Modern	Norwegian sea	**NORExIntrog**	35
		Eastern Mediterranean	**EMED**	10
		Central Mediterranean	**CMED**	10
		Western Mediterranean	**WMEDExIntrog**	9
		Gulf of Mexico	**GOM**	10
		All modern Atlantic bluefin locations	**modernExIntrog**	74
	Ancient	Jortveit, Norway	**Norway_3000BCE_ExIntrog**	23
		Sardinia, Italy	**Sardinia_1500_1700CE_ExIntrog**	14
		Istanbul, Turkey	**Istanbul_800_1200CE_ExIntrog**	17
		Sicily, Italy	**Sicily_900_1200CE_ExIntrog**	8
		Cádiz, Spain	**Gibraltar_100CE**	4
		Conil de la Frontera, Spain	**Gibraltar_1755CE**	7
		Istanbul, Turkey	**Istanbul_1941CE**	1
		Marseille, France	**Marseille_1800CE**	8
		Zliten, Libya	**Zliten_1925CE**	20
		All ancient excavation locations	**AncientExIntrog**	102
	Both modern and ancient	All modern and ancient Atlantic bluefin locations	**AllExIntrog**	176
Datasets with jointly called and filtered outgroup species	All samples in **AllABFT** + All albacore samples + All Pacific bluefin samples	All Atlantic bluefin locations + Bay of Biscay (albacore) + Nansei Islands (Pacific bluefin)	**All_ALB_PBFT**	202

In the table above, the following datasets were used for population genomic analyses:

- AllABFT: Used for LociMissingness analyses (Figure S5) and calculation of ΦST and d_{xy} (Figure 3B). No outgroup.
- All_ALB_PBFT: Used for interspecific PCA (Figure 2A) with no outgroup. It was also used for haplotype network (Figure 2C) and ML and Bayesian phylogenies (Figure 2D and Figure S6) using one katsuwonus pelamis as outgroup (NCBI Reference Sequence: NC_005316.1)
- AllExIntrog: Used for intraspecific PCA (Figure S8) and calculation of ΦST and d_{xy} (Figure 3A) with no outgroup. It was also used for intraspecific haplotype network (Figure S9), as well as ML and Bayesian phylogenies (Figure S10) using one Pacific bluefin as outgroup (NCBI Reference Sequence: NC_008455.1)

All other datasets were only used for the calculation of population genomic statistics (Table S15).

*Table S15: Population genomic statistics of the separately called and filtered datasets. N = number of samples, hD = haplotype diversity, Nh = number of haplotypes, S = number of segregating sites, π = nucleotide diversity, TD = Tajima's D. Significance levels (**=0.01, *=0.05, n.s.=not significant) are indicated for the TD values. Datasets containing introgressed samples have been highlighted in beige color.*

Subset	N	hD	Nh	S	π	TD	π(bs)	TD(bs)
AllABFT_mt	186	0.998	160	809	0.0033	-3.23 (**)	0.0027	-2.49
AllExIntrog_mt	175	0.999	158	475	0.0009	-3.23 (**)	0.0007	-2.82
modernABFT_mt	78	0.998	72	699	0.0035	-2.14 (*)	0.0035	-1.18
modernExIntrog_mt	74	0.999	70	300	0.0012	-2.49 (*)	0.0011	-1.20
AncientAll_mt	108	0.998	97	710	0.0034	-3.37 (**)	0.0024	-3.42
AncientExIntrog_mt	101	0.997	90	332	0.0008	-3.37 (**)	0.0005	-3.45
NORAll_mt	38	0.997	36	621	0.0049	-1.73 (n.s.)	0.0050	-0.92
NORExIntrog_mt	35	0.998	34	187	0.0012	-2.10 (*)	0.0012	-0.85
WMEDAll_mt	10	1.000	10	477	0.0060	-2.14 (*)	0.0060	-1.28
WMEDExIntrog_mt	9	1.000	9	74	0.0011	-1.71 (n.s.)	0.0011	-1.21
EMED_mt	10	1.000	10	90	0.0013	-1.59 (n.s.)	0.0013	-0.93
CMED_mt	10	1.000	10	90	0.0012	-1.87 (n.s.)	0.0012	-1.21
GOM_mt	10	1.000	10	78	0.0010	-2.17 (*)	0.0010	-1.58
Norway_3000BCE_All	24	1.000	24	556	0.0046	-3.91 (**)	0.0029	-3.68
Norway_3000BCE_ExIntrog	23	1.000	22	201	0.0012	-3.92 (**)	0.0008	-3.65
Sardinia_1500_1700CE_All	15	1.000	15	504	0.0042	-3.31 (**)	0.0035	-2.46
Sardinia_1500_1700CE_ExIntrog	14	1.000	14	95	0.0009	-3.47 (**)	0.0007	-2.65
Istanbul_800_1200CE_All	19	1.000	19	542	0.0054	-2.90 (**)	0.0049	-1.94
Istanbul_800_1200CE_ExIntrog	17	1.000	17	85	0.0009	-3.04 (**)	0.0007	-2.01
Sicily_900_1200CE_All	10	1.000	10	411	0.0062	-4.18 (**)	0.0037	-4.15
Sicily_900_1200CE_ExIntrog	8	1.000	8	43	0.0006	-4.55 (**)	0.0003	-4.64
Gibraltar_100CE	4	1.000	4	27	0.0008	-0.63 (n.s.)	n.a.	n.a.
Gibraltar_1755CE	7	1.000	7	30	0.0003	-5.17(**)	0.0001	-6.27
Istanbul_1941CE	1	n.a.	1	0	n.a.	n.a.	n.a.	n.a.
Marseille_1800CE	8	1.000	8	40	0.0006	-2.96 (**)	0.0005	-2.70
Zliten_1925CE	20	1.000	20	111	0.0008	-3.75 (**)	0.0006	-3.38

Section 3: Supplementary Figures

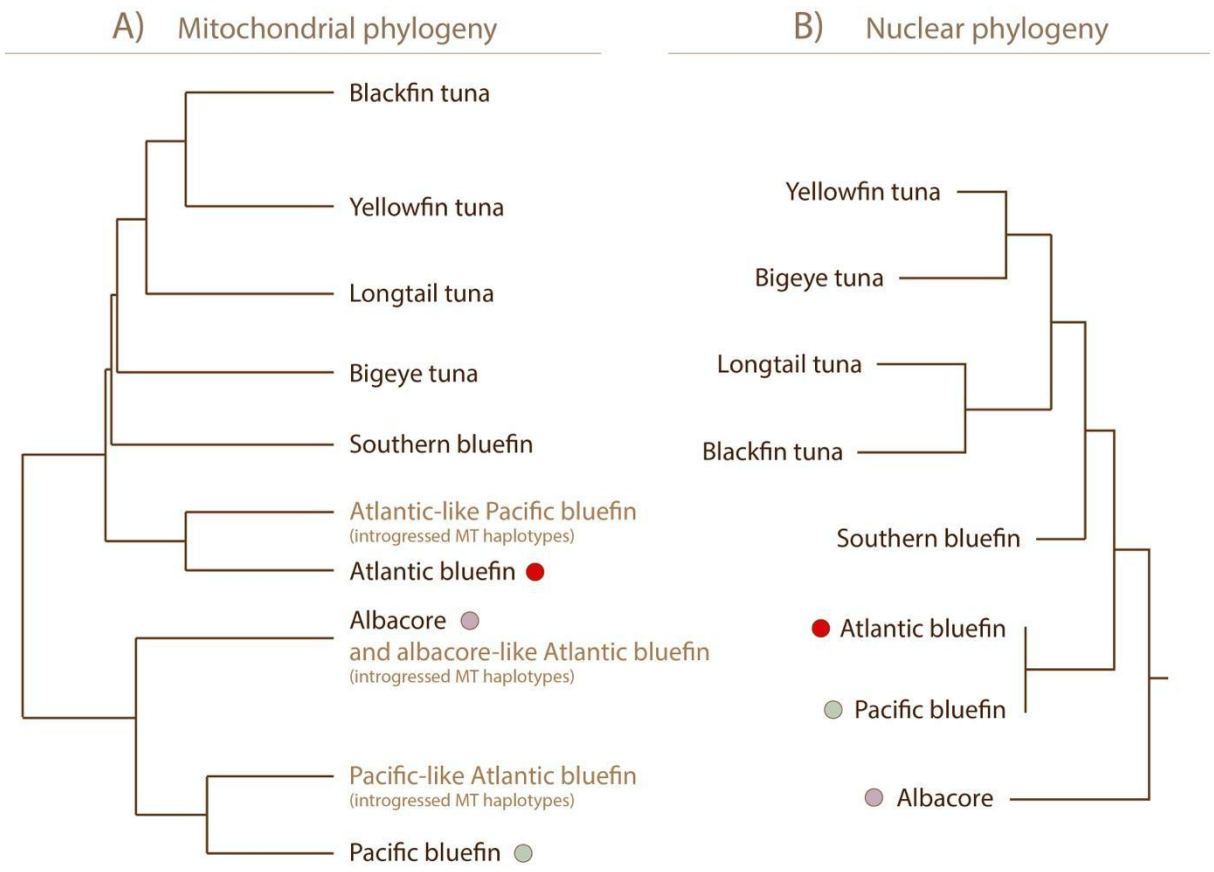

Figure S1: Thunnus phylogenies based on A) the mitochondrial control region adapted from Viñas & Tudela (2009) and B) genome-wide nuclear markers adapted from Díaz-Arce et al. (2016). Tip labels in light brown represent introgressed mitochondrial sequences. The colored circles mark species presented in this study.

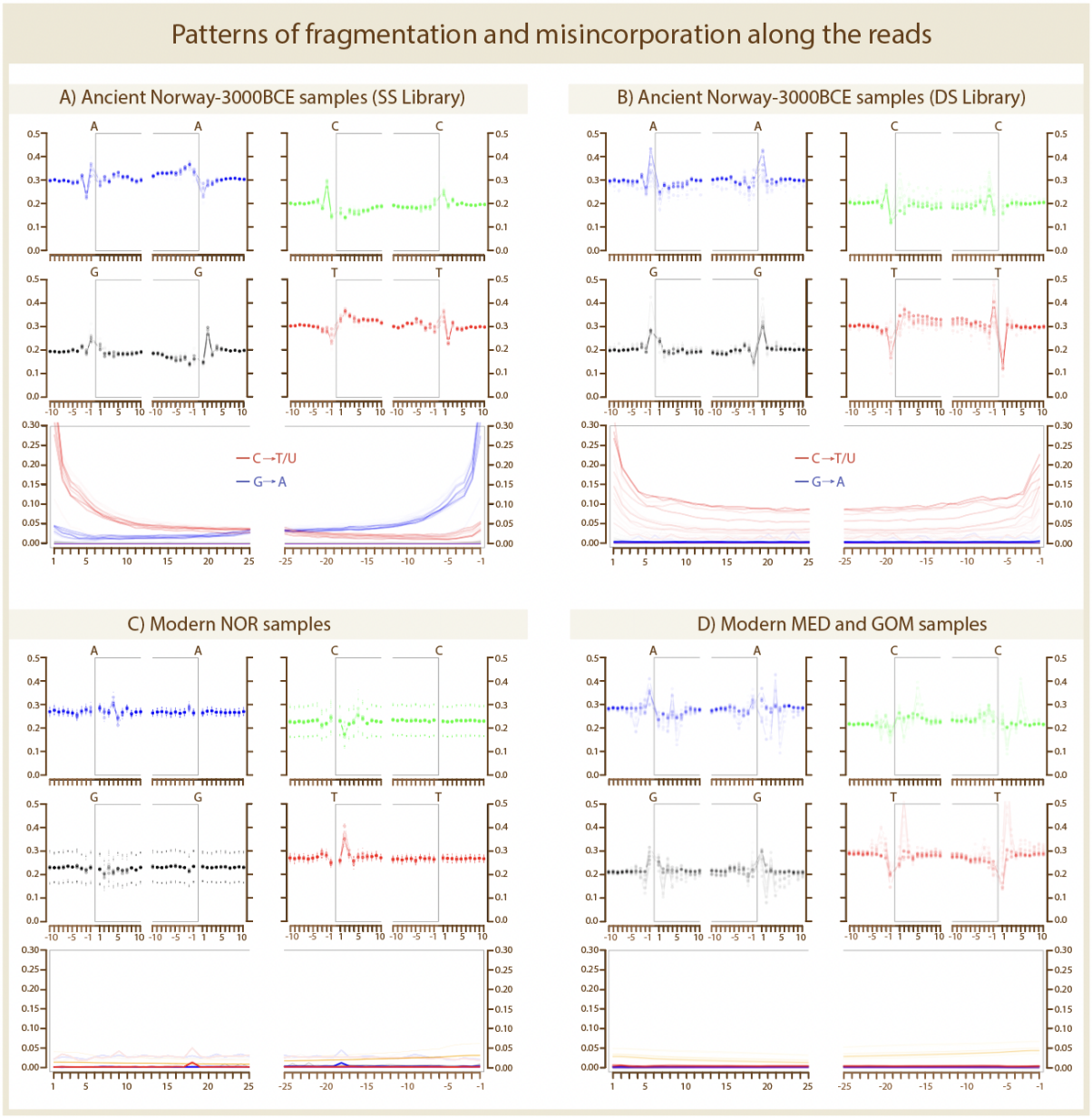

Figure S2: Fragmentation (upper panels) and misincorporation (lower panels) plots from mapDamage v.2.0.9. The fragmentation plots show the base frequency inside and surrounding the read, where the grey box indicates the location of where the reads have mapped to the reference. The misincorporation plots show the rate of substitutions along the positions of the read ends, relative to the reference (Red: C to T. Blue: G to A. Grey: All other substitutions. Green: Deletions. Purple: Insertions. Orange: Soft-clipped bases).

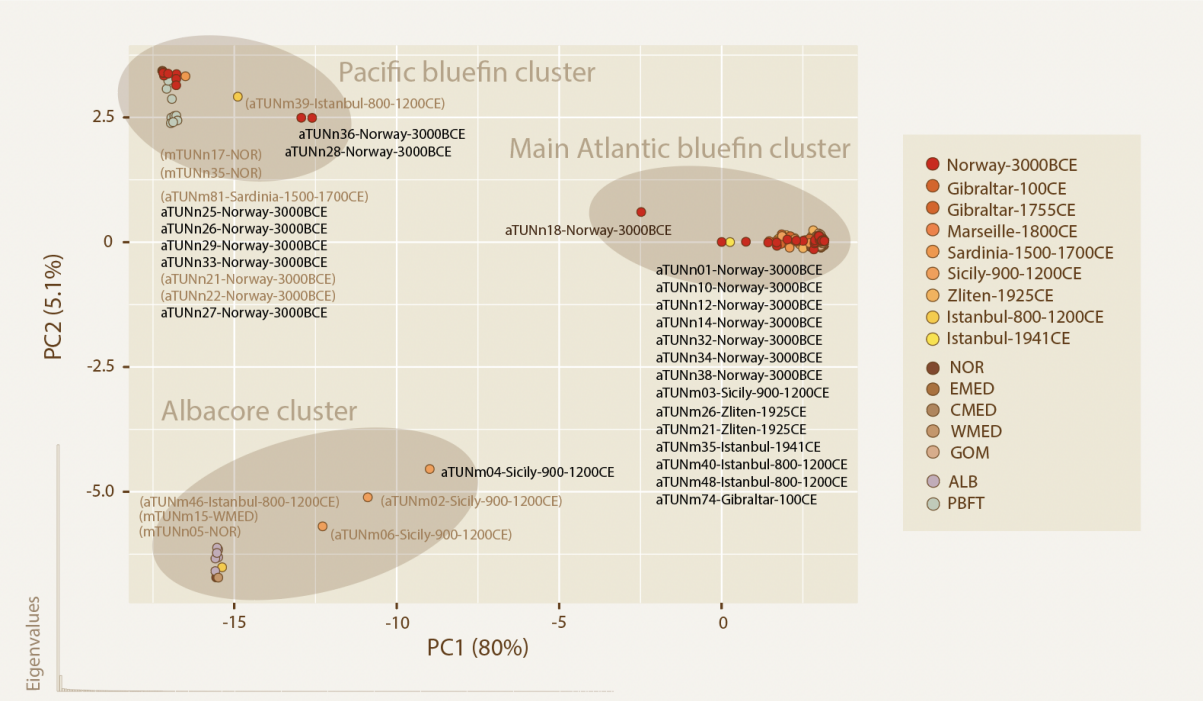

Figure S3: PCA of all samples included in the exploratory analysis, prior to omission of identical- and high missingness samples. The plot shows an interspecific PCA. Samples that were excluded from subsequent population genomic analyses are marked with the sample name in dark brown. Sample names in parentheses indicate diverging samples that were kept, but taken into account as introgressed haplotypes, in the population genomic analyses.

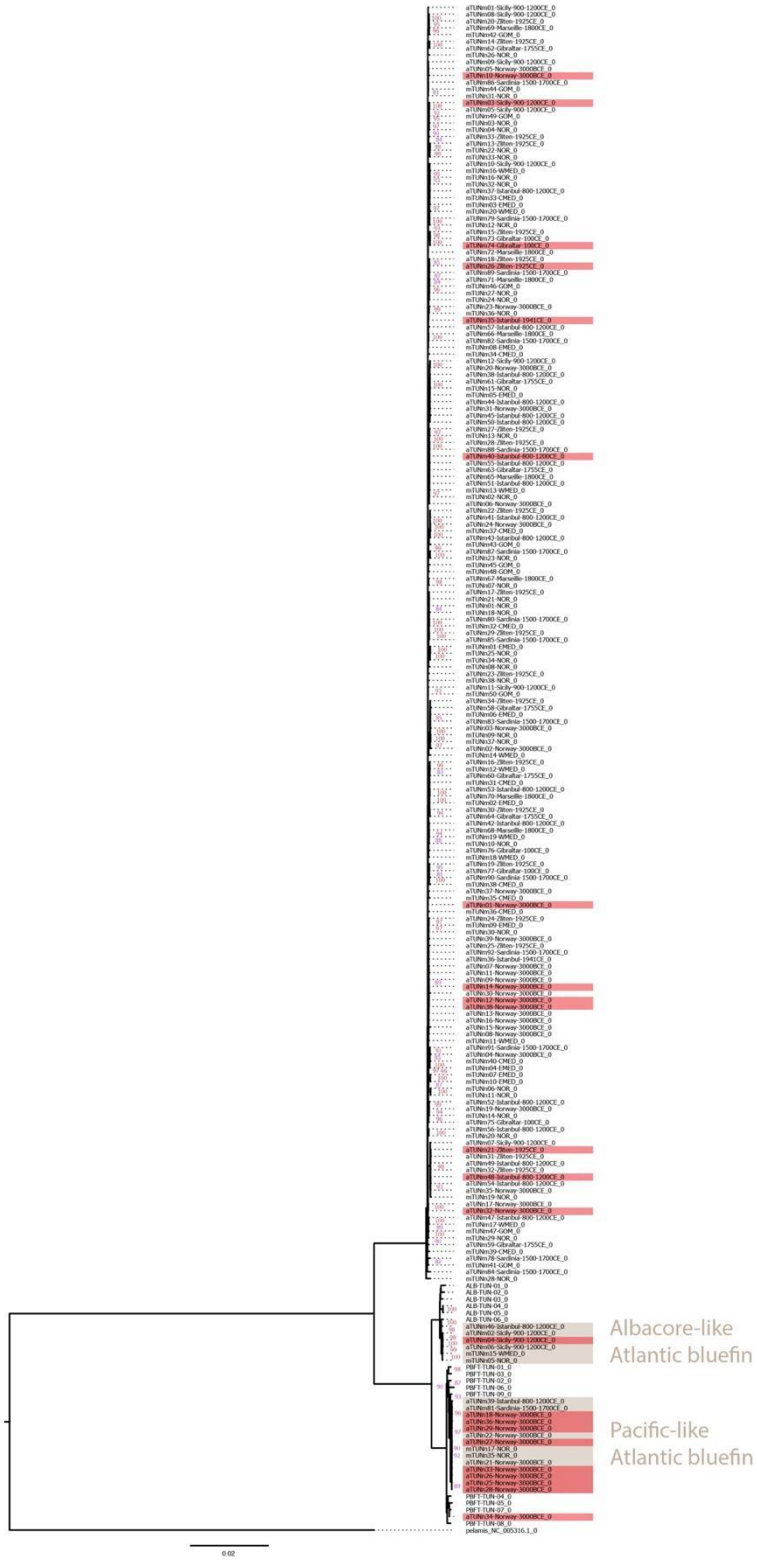

Figure S4: ML phylogeny of all samples included in the exploratory analysis, prior to omission of identical- and high missingness samples. Bootstrap values over 80 are shown in pink. Samples that were excluded from subsequent population genomic analyses are highlighted in red. Samples highlighted in brown indicate diverging samples that were kept, but taken into account as introgressed haplotypes, in the population genomic analyses.

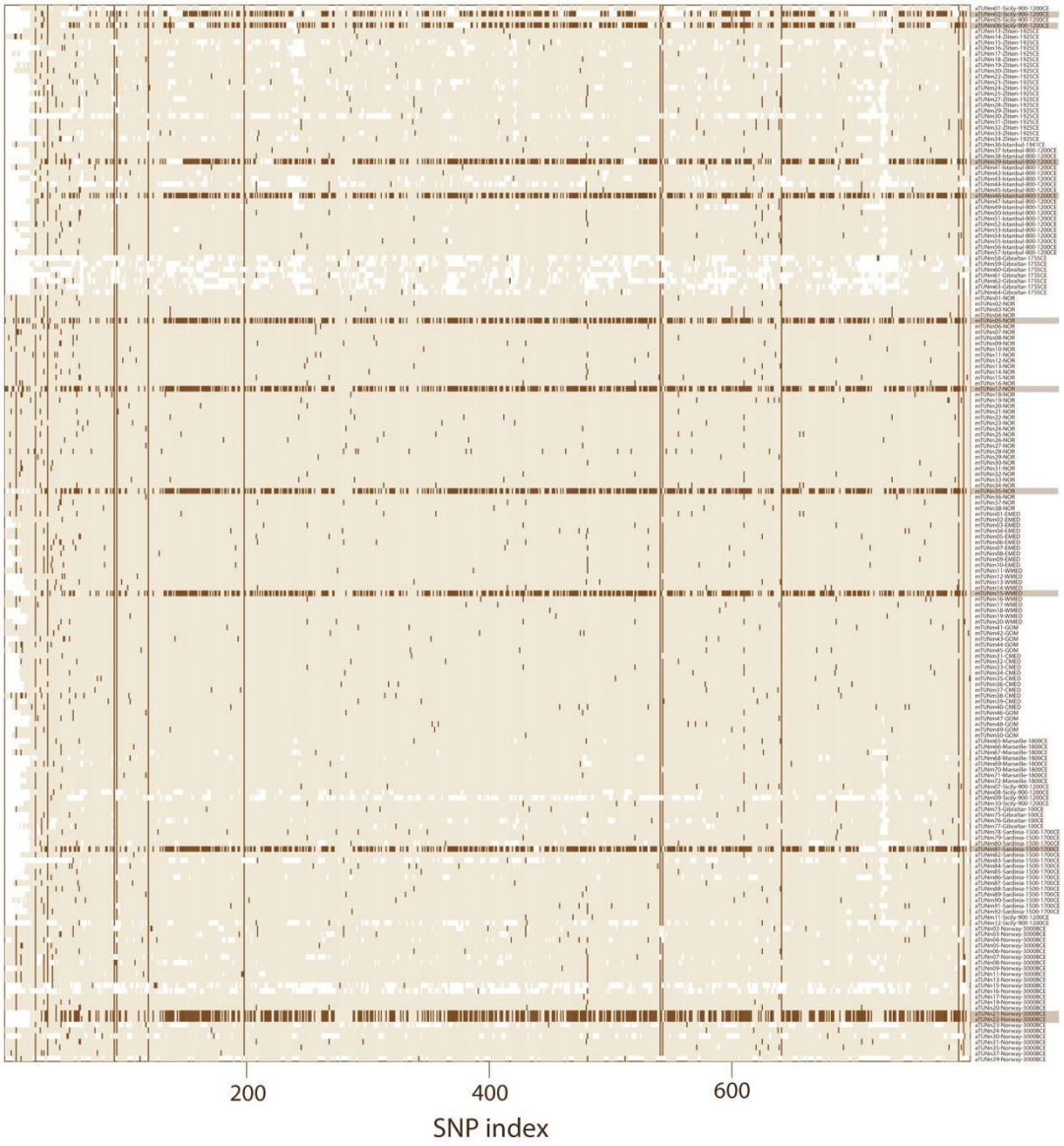

Figure S5: Missing loci (white) and the presence of second alleles (dark brown) across the Atlantic bluefin samples (dataset: AllABFT). The 11 specimens that were identified with introgressed MT genomes have a high number of divergent alleles when compared to the Atlantic bluefin reference genome.

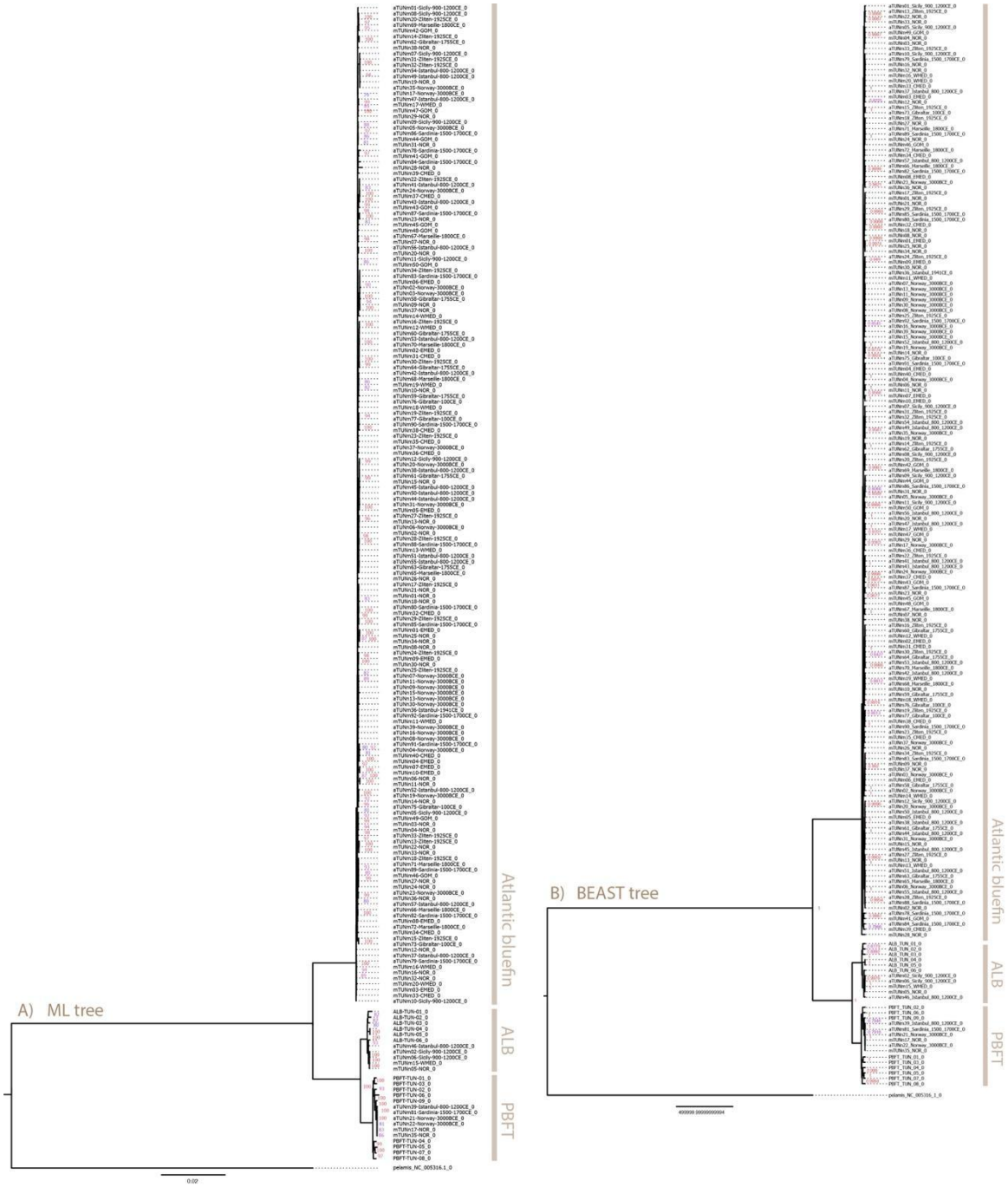

Figure S6: ML and Bayesian phylogenies of all samples included in population genomic analyses (dataset: All_ALB_PBFT) using Skipjack tuna (Katsuwonus pelamis) as outgroup. Bootstrap values over 80 and posterior probability values over 0.8 are shown in pink in A) and B) respectively. Species clades are highlighted in brown.

p-values for PHIst Excluding introgressed individuals

	Sicily_900_1200CE	Zliten_1925CE	Istanbul_1941CE	Istanbul_800_1200CE	Gibraltar_1755CE	Marseille_1800CE	Gibraltar_100CE	Sardinia_1500_1700Cl	Norway_3000BCE	EMED	WMED	CMED	GOM	NOR
Sicily_900_1200CE	*													
Zliten_1925CE	0.96680+-0.0073	*												
Istanbul_1941CE	0.99902+-0.0002	0.99902+-0.0002	*											
Istanbul_800_1200CE	0.77539+-0.0143	0.60938+-0.0149	0.75684+-0.0145	*										
Gibraltar_1755CE	0.07520+-0.0097	0.91504+-0.0085	0.48633+-0.0154	0.59961+-0.0155	*									
Marseille_1800CE	0.50977+-0.0173	0.57422+-0.0177	0.89160+-0.0104	0.45312+-0.0153	0.40039+-0.0165	*								
Gibraltar_100CE	0.69629+-0.0182	0.88965+-0.0102	0.81348+-0.0111	0.45996+-0.0163	0.28516+-0.0150	0.71875+-0.0132	*							
Sardinia_1500_1700CE	0.85840+-0.0096	0.57227+-0.0137	0.88184+-0.0080	0.10938+-0.0100	0.65625+-0.0145	0.70996+-0.0160	0.81934+-0.0101	*						
Norway_3000BCE	0.86133+-0.0090	0.64355+-0.0171	0.56348+-0.0152	0.27539+-0.0160	0.99023+-0.0032	0.31836+-0.0136	0.56445+-0.0150	0.34961+-0.0141	*					
EMED	0.58105+-0.0113	0.19922+-0.0103	0.99902+-0.0002	0.12012+-0.0080	0.45215+-0.0165	0.47461+-0.0147	0.56055+-0.0129	0.58984+-0.0170	0.36816+-0.0152	*				
WMED	0.73242+-0.0139	0.26074+-0.0143	0.91211+-0.0085	0.42383+-0.0167	0.93652+-0.0082	0.84863+-0.0092	0.91504+-0.0082	0.60156+-0.0173	0.34277+-0.0169	0.50391+-(	*			
CMED	0.99219+-0.0027	0.56934+-0.0160	0.99902+-0.0002	0.39941+-0.0137	0.70801+-0.0159	0.88965+-0.0117	0.99316+-0.0022	0.97852+-0.0041	0.63867+-0.0133	0.79199+-(	0.78223+-	*		
GOM	0.84570+-0.0118	0.63477+-0.0130	0.79395+-0.0130	0.04980+-0.0061	0.79883+-0.0116	0.80664+-0.0107	0.85156+-0.0117	0.73828+-0.0144	0.40039+-0.0133	0.41211+-(	0.31348+-	0.8056	*	
NOR	0.98633+-0.0046	0.43262+-0.0170	0.93945+-0.0087	0.09863+-0.0092	0.46875+-0.0190	0.87109+-0.0102	0.70215+-0.0116	0.70801+-0.0144	0.04395+-0.0050	0.65820+-(	0.35059+-	0.6289	0.76270+-0.0135	

p-values for PHIst Including introgressed individuals

	Sicily_900_1200CE	Zliten_1925CE	Istanbul_1941CE	Istanbul_800_1200CE	Gibraltar_1755CE	Marseille_1800CE	Gibraltar_100CE	Sardinia_1500_1700Cl	Norway_3000BCE	EMED	WMED	CMED	GOM	NOR
Sicily_900_1200CE	*													
Zliten_1925CE	0.00391+-0.0023	*												
Istanbul_1941CE	0.99902+-0.0002	0.99902+-0.0002	*											
Istanbul_800_1200CE	0.35938+-0.0125	0.38867+-0.0145	0.79590+-0.0101	*										
Gibraltar_1755CE	0.49414+-0.0147	0.65527+-0.0126	0.52051+-0.0166	0.99902+-0.0002	*									
Marseille_1800CE	0.11230+-0.0099	0.61230+-0.0135	0.89453+-0.0122	0.31055+-0.0102	0.26562+-0.0142	*								
Gibraltar_100CE	0.09570+-0.0098	0.93066+-0.0092	0.81934+-0.0104	0.80566+-0.0137	0.14551+-0.0089	0.77148+-0.0120	*							
Sardinia_1500_1700CE	0.30859+-0.0103	0.41113+-0.0166	0.74707+-0.0139	0.84570+-0.0099	0.99902+-0.0002	0.60254+-0.0114	0.75195+-0.0151	*						
Norway_3000BCE	0.33398+-0.0164	0.10156+-0.0102	0.47168+-0.0132	0.89062+-0.0095	0.95605+-0.0056	0.15234+-0.0110	0.43652+-0.0135	0.52344+-0.0133	*					
EMED	0.00098+-0.0010	0.23730+-0.0126	0.99902+-0.0002	0.14258+-0.0133	0.45215+-0.0175	0.46094+-0.0179	0.71875+-0.0107	0.52637+-0.0143	0.09668+-0.0090	*				
WMED	0.39258+-0.0156	0.33105+-0.0132	0.99902+-0.0002	0.82520+-0.0102	0.99902+-0.0002	0.93555+-0.0072	0.97168+-0.0043	0.97266+-0.0056	0.66797+-0.0123	0.39160+-(	*			
CMED	0.00293+-0.0016	0.62012+-0.0167	0.99902+-0.0002	0.16992+-0.0115	0.72461+-0.0135	0.94238+-0.0064	0.99805+-0.0010	0.65332+-0.0159	0.09668+-0.0110	0.78125+-(	0.41113+-	*		
GOM	0.00098+-0.0010	0.65430+-0.0159	0.81641+-0.0102	0.12109+-0.0102	0.73145+-0.0149	0.83984+-0.0126	0.90918+-0.0081	0.53418+-0.0159	0.08008+-0.0078	0.36523+-(	0.36816+-	0.7285	*	
NOR	0.19043+-0.0120	0.54395+-0.0175	0.94336+-0.0078	0.80273+-0.0118	0.99902+-0.0002	0.98828+-0.0036	0.96973+-0.0046	0.98926+-0.0029	0.57715+-0.0159	0.37598+-(	0.80762+-	0.2587	0.50293-	*

Figure S7: ΦST P-values from Arlequin for the AllExIntrog and AllABFT datasets, corresponding to Figure 3A) and 3B) respectively. Significant p-values are marked in green. After correcting for multiple testing (Bonniferoni correction), none of the p-values remained significant.

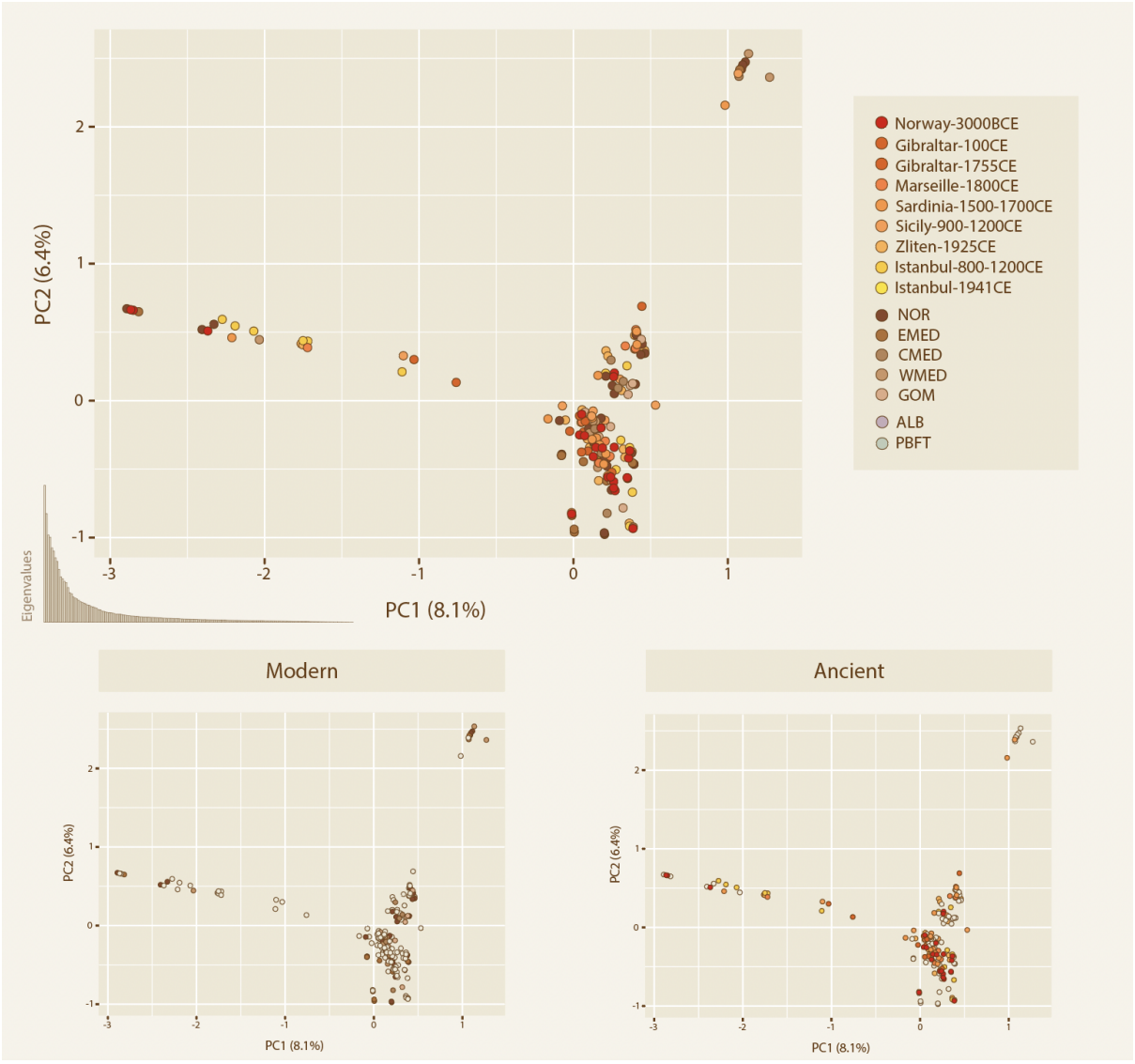

Figure S8: PCA of all non-introgressed Atlantic bluefin individuals (dataset: AllExIntrog). The ancient and modern samples are highlighted in the bottom panel. Eigenvalues are shown in the left corner of the upper panel.

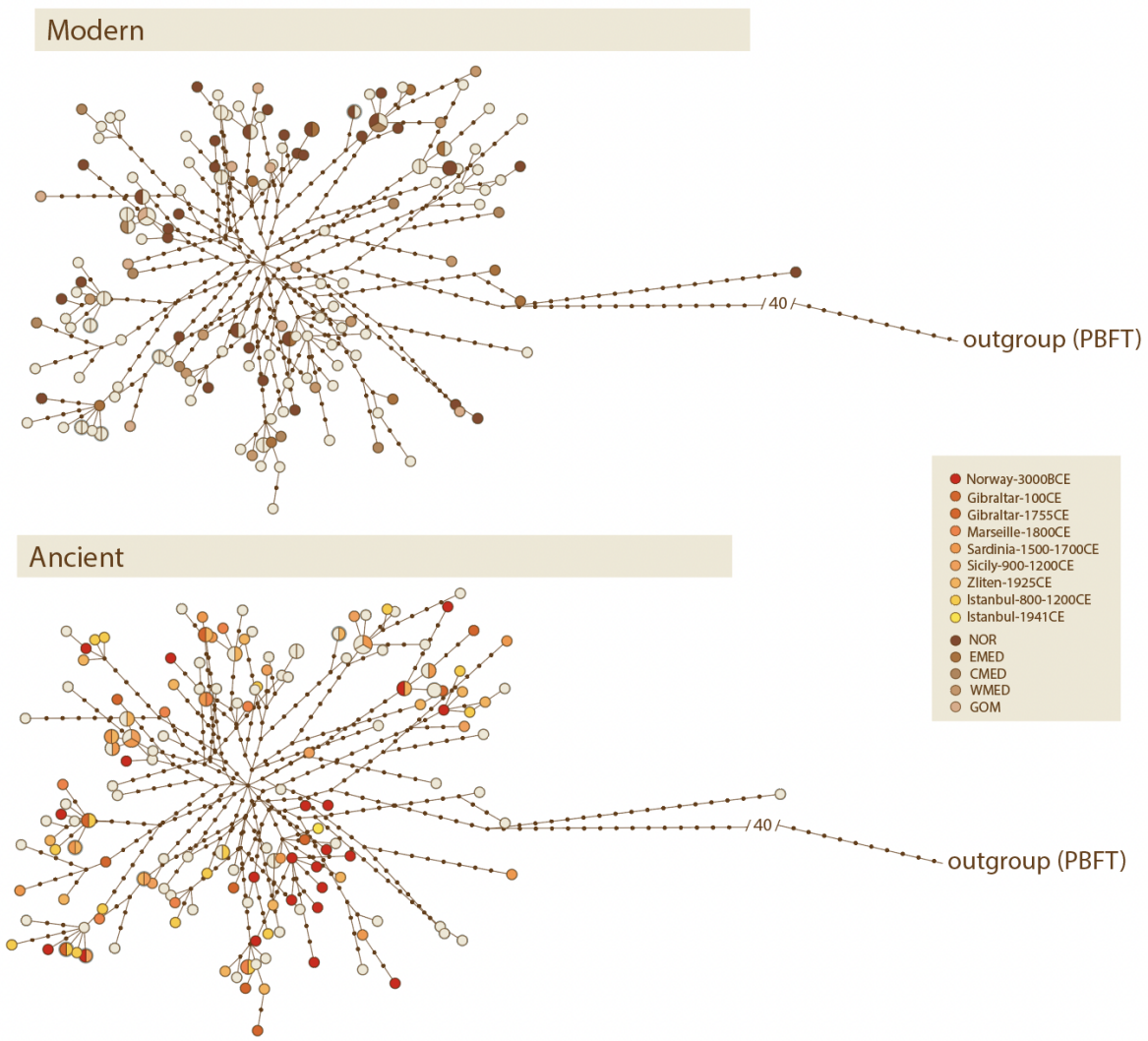

Figure S9: Haplotype network of all non-introgressed Atlantic bluefin individuals, using dataset AllExIntrog and Pacific bluefin (Thunnus orientalis) as outgroup. Each node represents a unique haplotype.

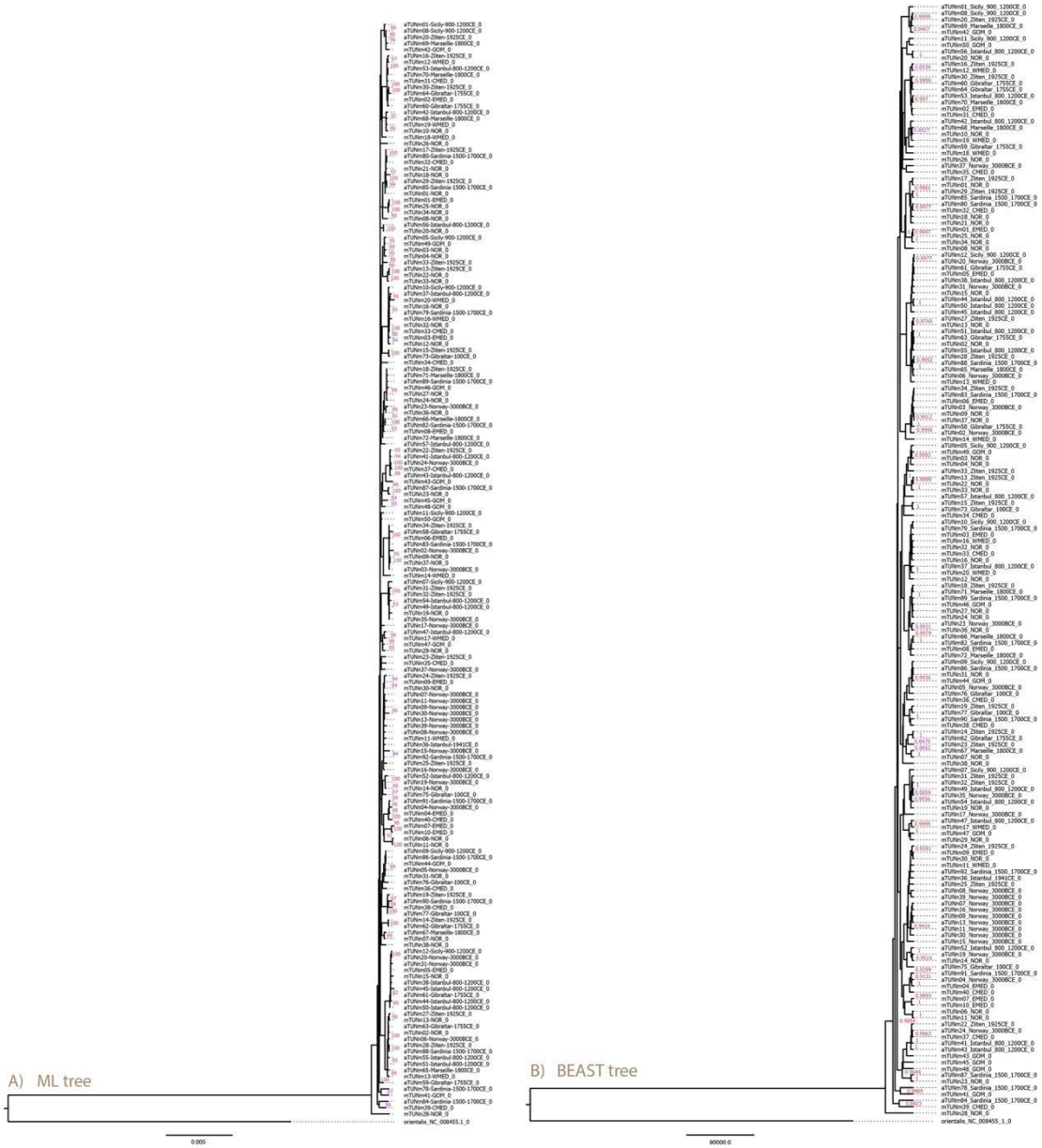

Figure S10: ML and Bayesian phylogenies of all samples included in population genomic analyses (dataset: AllExIntrog) using Pacific bluefin (Thunnus orientalis) as outgroup. Bootstrap values over 80 and posterior probability values over 0.8 are shown in pink in A) and B) respectively.